THE OPEN CLUSTERS
NGC 6604 AND NGC 6704

Douglas W. Forbes

A thesis submitted as
partial requirement
for the degree of
Master of Science
from
St. Mary's University

Department of Astronomy
Saint Mary's University
1977

Table of Contents

Acknowledgements

I would like to express my thanks to the following:

Dr. D.L. DuPuy, for suggesting this thesis topic, for acting as my supervisor, and for providing the opportunity to do a bit of "real" (observational) astronomy. His many helpful suggestions and criticisms proved invaluable. Without his assistance, this thesis would simply not have been possible.

Dr. G.A. Welch, for obtaining and permitting the use of his excellent photoelectric photometry and plate material, which were essential to the thesis.

Dr. G.C. Kilambi, for sharing his expertise on open clusters.

Dr. R.F. Garrison, for telescope time at the University of Toronto Las Campanas Observatory in July, 1976.

Abstract

At the suggestion of Dr. D.L. DuPuy, the young open clusters NGC 6604 and NGC 6704 were observed in the UBV wide-band system in order to obtain improved colour-magnitude diagrams and estimates of distance.

A short introduction serves to present basic information and review previous studies of the two clusters, and to demonstrate their potential importance in determining the spiral structure of the Galaxy near the Sun.

The second and third chapters describe the photoelectric and photographic observations and reductions, including a section on difficulties encountered with the iris photometer used to measure the plates. A section on results contains two appendices, giving approximately 100 UBV measures in the fields of both clusters.

The methods of determining reddening corrections, cluster membership, and distance moduli are discussed in some detail in Chapter 4.

Chapter 5 is a discussion of the colour-magnitude diagrams for both clusters. Age estimates are also derived; NGC 6604 is found to have an estimated age of ~4 million years, and NGC 6704 an estimated age of 20 million years.

The relation of both clusters to the local spiral structure is the topic of Chapter 6, but due to the small sample, there is little new information gained.

A discussion of possible future work towards determining the spiral structure between galactic longitudes $\ell = 20°-70°$ at distances greater than 2 kpc from the Sun, and investigating the possible pre-main-sequence stars which may be members of NGC 6604, concludes the study.

1.) INTRODUCTION

The recognition of the Milky Way as one galaxy among many other such "island universes" was a fundamental revelation in the history of astronomy. Once the Milky Way could be considered as a system of stars not unlike an object such as the Andromeda galaxy, it became possible to look for a similar sort of spiral structure in the vicinity of the Sun.

In the 1950's, the work of Baade and Mayall (1951) on the association of H II regions with the spiral arms of M 31 and the studies of Morgan, Sharpless, and Osterbrock (1952) concerning the distribution of early-type stars associated with the nearer H II regions in the Galaxy gave the first real indication of local spiral structure in the Milky Way. Since that time a good deal of work has gone into the search for spiral structure near the Sun.

Spiral structure in the Galaxy may be determined, in principle, by four different methods (Schmidt-Kaler, 1971); one of these methods involves determining the positions and distances of objects which are reliable spiral tracers. Rohlfs (1967) and McCuskey (1970) have shown that H II regions, early-type Be stars, and early-type open clusters and associations are among the best. Numerous investigations have resulted in a distribution similar to that given by Becker and Fenkart (1970), with the following apparently well-established features (Schmidt-Kaler, 1971):

Spiral Feature	Galactic Longitude	Distance
Local (Orion)	60° ... 210°	Sun at inside edge
+I (Per)	90° ... 140°	2-3 kpc
-I (Sgr)	330° ... 30°	2 kpc
+II (Car-Cen)	285° ... 305°	1.5-5 kpc
-II (Nor-Sct)	325° ... 30°	4 kpc

The question has been raised by several studies (e.g. Humphreys, 1976) as to whether the Local feature is truly a major spiral arm or simply an inter-arm feature. It may be possible to resolve this question optically by attempting to follow the Local, +I (Per), and -I (Sgr) features out to greater distances from the Sun. Recent work (Bok, 1970; Humphreys, 1976; FitzGerald and Moffat, 1974) has tended to concentrate on the region between galactic longitudes $\ell = 240° - 340°$. The region between $\ell = 20°$ and $\ell = 90°$, however, seems to have suffered from some perhaps not wholly justified neglect.

Inspection of wide-angle photographs of this region of the Milky Way indicate a possible reason for a paucity of observations of spiral tracers between $\ell = 20° - 90°$ — obscuration. This is well shown in the work of Lynds (1962). The interstellar absorption serves to make any optical spiral tracers less evident and more prone to uncertainties in distance estimates. It is the effect on distance determination that is critical in the investigation of the spiral structure in this direction, along either the Local or -I feature. The uncertainties in distances are not altogether surprising when one considers the visual absorption given by Lynds (1968) for various dark nebulae located between $\ell = 20°$ and 90°: from 1 to 4 magnitudes.

Two open clusters, NGC 6604 and NGC 6704 are listed in the Catalogue of Star Clusters and Associations (Alter, Ruprecht, and Vanýsek, 1970) as lying within the region between $\ell = 20°-90°$, whose spectral types (O and B) are indicative of youth, and which have rather uncertain distance estimates. Basic information on the two clusters is given in Table I.

NGC 6604 is a member of the association Ser OB 2, for which Sharpless (1965) gives a distance of 2.0 kpc. This appears to have been an accepted value until the photometry of Moffat and Vogt (1975) who derive a distance of 1.64 kpc (no quoted uncertainty). This result is at odds with previous estimates of both the cluster and the associated H II region distances. Miller (1968), for example, gives a distance of 1.9 kpc and Georgelin, et al. (1973) give a photometric distance of 2.05 kpc and a kinematice distance of 2.77 $\pm$ 0.42 kpc for the H II region, which is noted as S 54 in the catalogue of Sharpless (1955).

NGC 6704 is a rather faint cluster which has had relatively little previous study. The only known photometry is that of Grubbisich (1965) which was obtained photographically in the RGU system. Four plates each in R, G, and U were measured on the Basel iris-diaphragm photometer, with a photoelectric calibration scale taken from the nearby cluster M 11, which was included on the plates and for which Johnson, Sandage, and Wahlquist (1956)

TABLE I

Basic Cluster Information

Cluster	RA (1950)	Dec.			Type	Distance estimates	Sp. Type
NGC 6604	$18^h\ 15^m.3$	$-\ 12°\ 15'$	18°3	+ 1°7	I3p	0.7-4.4 kpc	05-7
NGC 6704	$18^h\ 48^m.2$	$-\ 05°\ 16'$	28°2	- 2°2	I3m	1.4-3.2 kpc	B2

(Data from Alter, Ruprecht, and Vanýsek, 1970) had published UBV measures. The transformation of the B and V magnitudes was done "nach den schon benutzten Formeln von Stock" (although no reference to Stock is given), with the following mean errors:

$\pm$ 0.05 ($\pm$ 0.08) mag in R

$\pm$ 0.04 ($\pm$ 0.06) mag in G

$\pm$ 0.07 ($\pm$ 0.09) mag in U

where the values in parentheses are valid for stars about 0.5 magnitudes above the measuring limit. No mention is made of possible trends or errors in the transformations from B and V to R and G. Grubbisich's criteria for cluster membership appear to be simply the locations of a given star on the G vs. (G-R) and G vs. (U-G) diagrams. The author is also not specific as to how the distance modulus or reddening was determined, although a main-sequence fitting procedure is implied. In short, there seems to be sufficient reason for a re-investigation of this cluster.

NGC 6704 is known to contain the eclipsing binary system FN Sct, an Algol-type variable with a period of $4\overset{d}{.}167153$ and a magnitude range (photographic) of 13.1 - 15.2 mag. (Bakos, 1950). No variables have as yet been found in NGC 6604, and no facilities were available for blinking the plates in this study. The <u>General Catalogue of Variable Stars</u> (Kukarkin, et al., 3rd ed. and supplements, 1969, 1974) was searched for variables near both clusters; none were found within 30 arc-minutes of NGC 6704: the eclipsing binary system CV Ser is within 45 arc-minutes of NGC 6604, but was not included in the field of any of the plates used in this study, so nothing can be said concerning possible cluster membership.

It was decided to observe these two clusters in the UBV wide-band system on the basis of i) the discordant distance estimates; ii) the lack of detailed photometry; iii) the possible youth of the clusters; and iv) the somewhat casual membership criteria for NGC 6704.

2.) PHOTOELECTRIC PHOTOMETRY

2.1 Observations

Preliminary photoelectric observations of NGC 6604 and NGC 6704 were obtained by Dr. Gary A. Welch in June of 1975. In order to obtain a more complete photoelectric sequence (for reasons which are explained in Chapter III), I was fortunate to obtain two weeks of dark-moon time in late July of 1976 at the Las Campanas Observatory in order to observe the two clusters, both photoelectrically and photographically, with the University of Toronto 61-cm telescope. Las Campanas Observatory is located at approximately 29° S, 71° W, at an altitude of 2250 meters. The 61-cm telescope is a Boller & Chivens Cassegrain with aluminum reflecting surfaces. This instrument was used for both the photoelectric and photographic observations. In addition to the observations of Dr. Welch in June of 1975, further photoelectric observations were made on two nights in July, 1976. These two nights, 19/20 and 20/21 July, were the only photometric-quality nights that occured in the two weeks from 19 July to 1 August.

2.2 Photoelectric Equipment

For all photoelectric observations, an RCA 1P21 photomultiplier cooled by dry ice was used with SSR (now Princeton Applied Research) model 1120 discriminator-amplifier and model 1110 counter. This photon-counting equipment has a nominal deadtime of 28 nanoseconds (Fernie, 1976); that is, this system is capable of a time resolution of photon arrival times down to 28 nsec. Observations of stars bright enough to produce a greater arrival rate of photons than this must be corrected for those pulses which are not counted because of coincidence in the arrival times. Several stars with a range of apparent V magnitude between 3.5 and 8.5 were observed to check on the necessity of making deadtime corrections. It was found that, for stars with V, B, and U magnitudes fainter than 7^m, the deadtime correction was smaller than 0.01 mag. Since the brightest program star observed had an apparent V magnitude of 7.51, no deadtime corrections were necessary. All observations were made with standard Johnson UBV filters.

2.3 Photoelectric Reductions

Because of the photon-counting mode, the bright Johnson standard stars were not observed. Instead, UBV values given by Landolt (1973) were employed for determining extinction and transformation coefficients. These coefficients were calculated using the general technique of Hardie (1962). A short summary of the method follows:

The extinction coefficients are given by:

$$\begin{aligned} k_v &= k'_v + k''_v(b-v)_o \\ k_{bv} &= k'_{bv} + k''_{bv}(b-v)_o \\ k_{ub} &= k'_{ub} + k''_{ub}(u-b)_o \end{aligned} \qquad (1)$$

where lower case letters u, b, v, are instrumental magnitudes; k is the extinction coefficient in magnitudes per air mass, k' the first order coefficient, and k" the second order term resulting from the variation of extinction with colour.

The term k''_v is taken to be negligible, and k''_{ub} is zero by definition. The air mass X is found from the relation

$$X = \sec z = (\sin\phi \sin\delta + \cos\phi \cos\delta \cos h)^{-1}$$

where ϕ is the observer's latitude and δ, h are the declination and hour angle of the star.

The extinction was determined from three to four observations of two close ($\leq 1'$) red and blue pairs over an air mass range of 1 to 2.5. The observations of extinction pairs and the associated air mass value were used to solve the following by method of linear least squares:

$$\begin{aligned} v_o &= v - k_v X \\ (b-v)_o &= (b-v) - k_{bv} X \\ (u-b)_o &= (u-b) - k_{ub} X \end{aligned} \qquad (2)$$

where v_o, $(b-v)_o$, $(u-b)_o$ are values corrected for extinction. These solutions yielded k_v, v_o, k_{bv}, $(b-v)_o$, k_{ub}, and $(u-b)_o$ for each star. These values were then used to solve equations (1) to find first and second order coefficients.

Nine standard stars were observed at least twice on 20/21 July with an air mass range of 1 to 2.5. The standard stars were corrected for extinction using the preliminary coefficients given above, and then fitted to the equations

$$\begin{aligned} V &= v_o + \epsilon(b-v)_o + \zeta_v \\ B-V &= \mu(b-v)_o + \zeta_{bv} \\ U-B &= \psi(u-b)_o + \zeta_{ub} \end{aligned} \qquad (3)$$

by the method of linear least squares to give preliminary values of the transformation coefficients and zero points.

To improve the determination of extinction, an iteration scheme (DuPuy, 1972) was employed. This iteration involves substituting equations (2) into (3) and rearranging:

$$\begin{aligned} \left\{(v-V) + \epsilon\,(b-v)_o\right\} &= k'_v(X) - \zeta_v \\ \left[\frac{\mu\,(b-v)}{1 + k''_{bv}X} - (B-V)\right] &= k'_{bv}\left(\frac{\mu X}{1 + k''_{bv}X}\right) - \zeta_{bv} \qquad (4) \\ \left\{\psi(u-b) - (U-B)\right\} &= k'_{ub}(\psi X) - \zeta_{ub} \end{aligned}$$

where capital letters stand for standard (i.e. Landolt) values of V, (B-V), and (U-B). Improved values of the first order extinction coefficients are the result of solving equations (4) by the method of linear least squares with preliminary values of ϵ, μ, and ψ and the instrumental magnitudes and colours uncorrected for extinction. These improved first order coefficients are then used to correct the instrumental values for extinction, and equations (3) are then re-employed to yield final values of transformation coefficients and zero points. Only one iteration was necessary. The final results for extinction and transformation coefficients and zero points are:

$$k_v = 0.129 \pm 0.026$$

$$k'_{bv} = 0.073 \pm 0.005$$

$$k''_{bv} = -0.018 \pm 0.037$$

$$k'_{ub} = 0.242 \pm 0.114$$

$\epsilon = 0.031$ $\mu = 0.936$ $\psi = 1.095$

$\zeta_v = 3.380$ $\zeta_{bv} = 1.023$ $\zeta_{ub} = -0.663$

The transformations to the UBV system were then:

$$V-v_o = 0.031(b-v)_o + 3.380$$

$$B-V = 0.936(b-v)_o + 1.023$$

$$U-B = 1.095(u-b)_o - 0.663$$

(see Figures 1, 2, and 3)

Residuals, in the sense

$$\Delta m = m_{std} - m_{obs}$$

were calculated and plotted versus air mass, colour, and magnitude (Figures 4 and 5). No significant trends were evident in these plots. The r.m.s. errors in the residuals are:

$$\Delta V = 0.022 \text{ mag}$$

$$\Delta(B-V) = 0.024 \text{ mag}$$

$$\Delta(U-B) = 0.040 \text{ mag}$$

The observations of 19/20 July were interrupted by clouds before a sufficient number of standard stars could be observed to satisfactorily determine the extinction coefficients. Therefore, the extinction coefficients of 20/21 July were used as preliminary values, and the DuPuy iteration scheme was employed to find final extinction coefficients and transformation coefficients and zero points for the observations of 19/20 July. The transformation coefficients and zero points, and the final values of extinction coefficients are then:

Figures 1, 2, and 3

Graphical representation of linear least squares solutions of the transformation equations (3), from data of 20/21 July, 1976. Lower-case letters indicate instrumental colours and magnitudes.

Figure 1

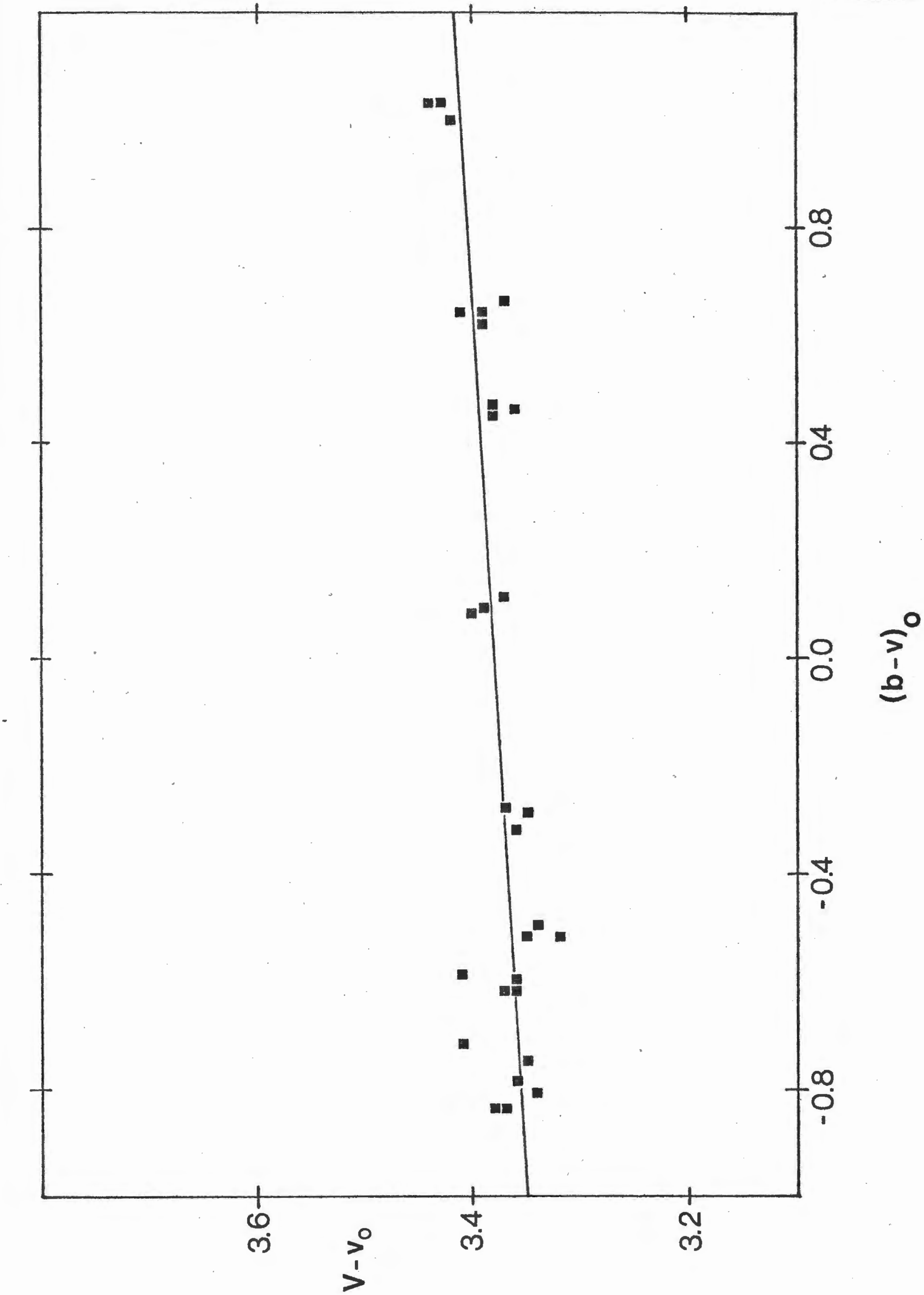

Figure 2

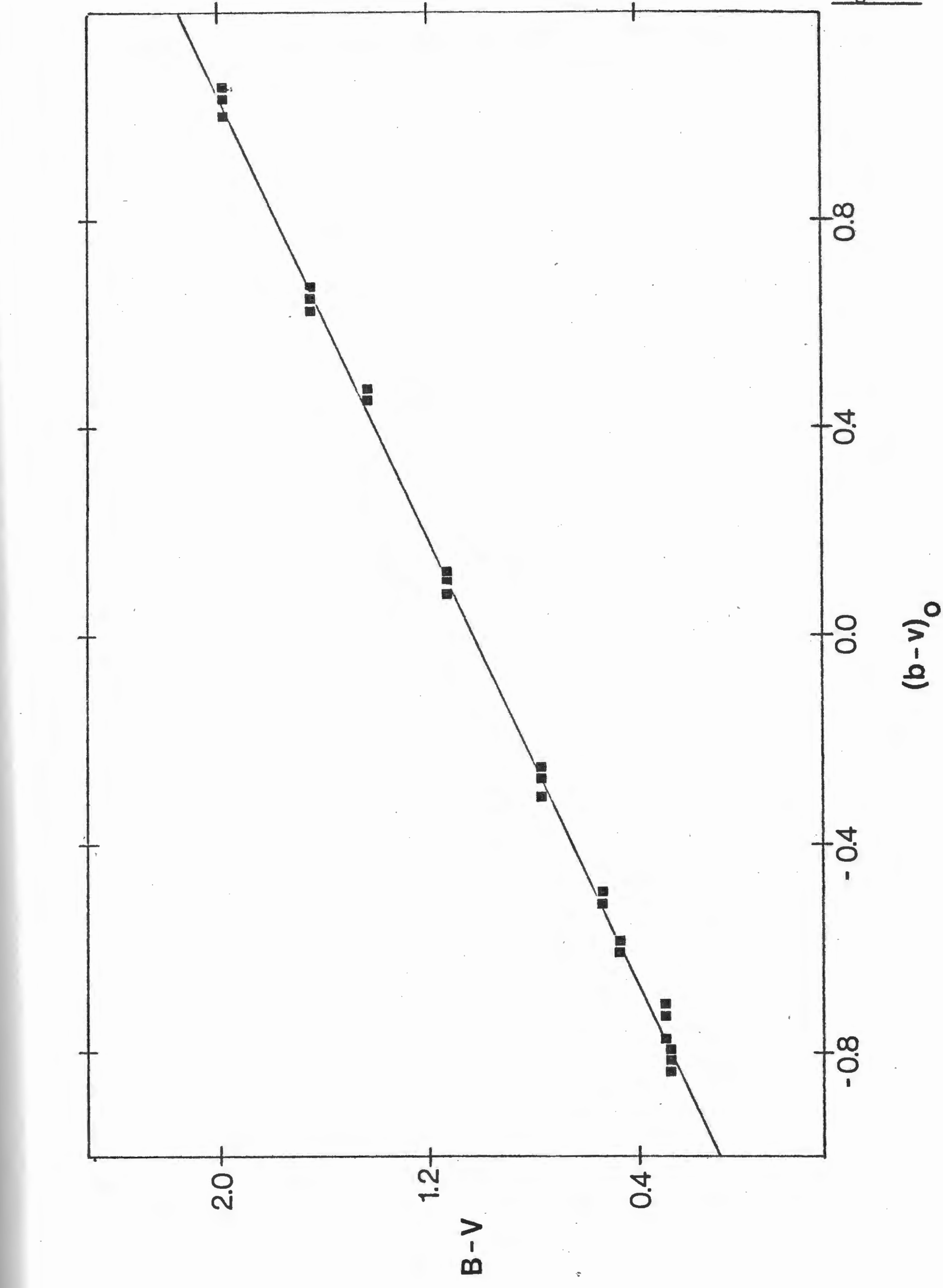

Figure 3

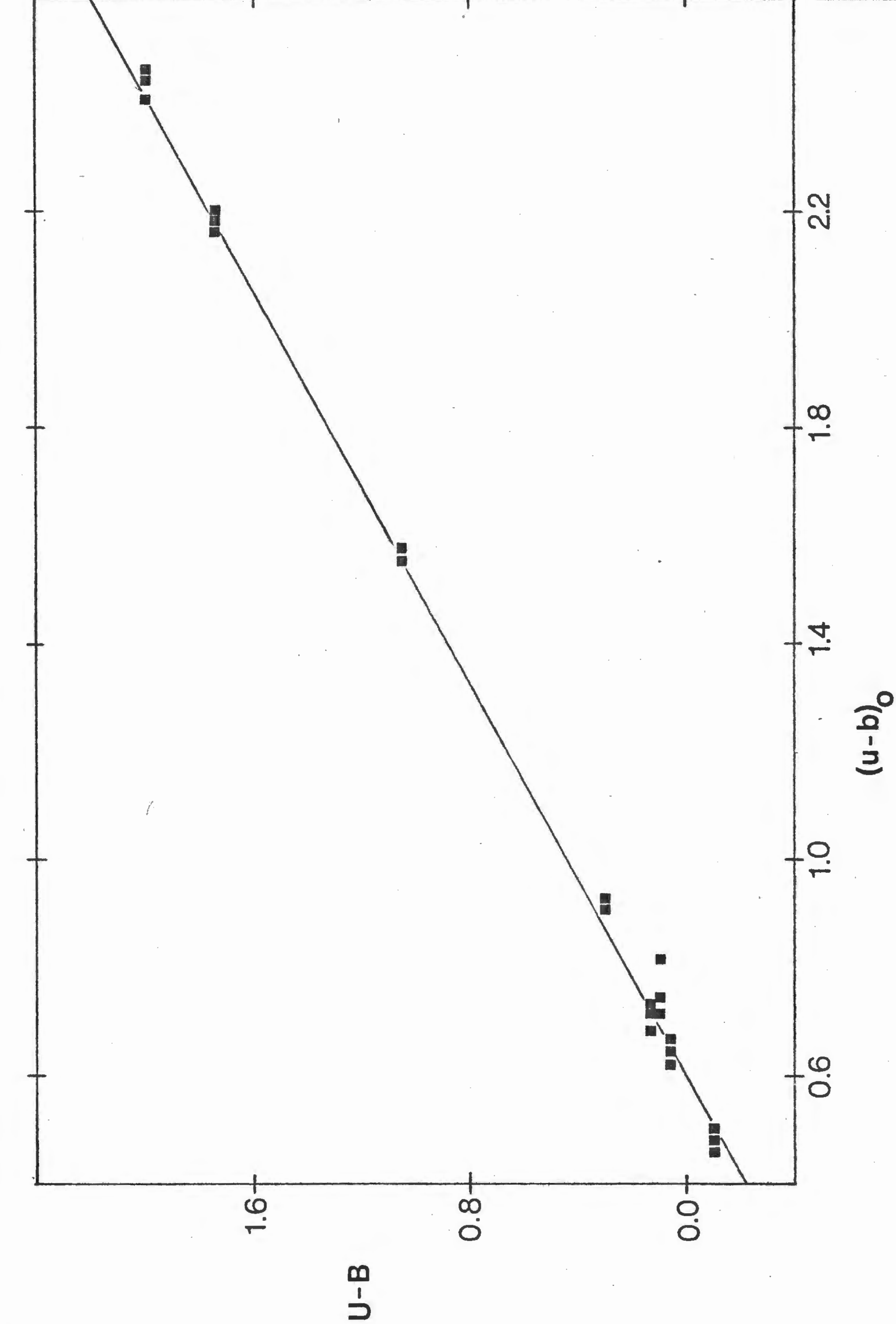

Figures 4 and 5

Differences between standard magnitudes and colours and photoelectric magnitudes and colours, in the sense $\Delta m = m_{std} - m_{pe}$, plotted versus air mass (Figure 4) and versus colour (Figure 5) for the data of 20/21 July, 1976.

Figure 4

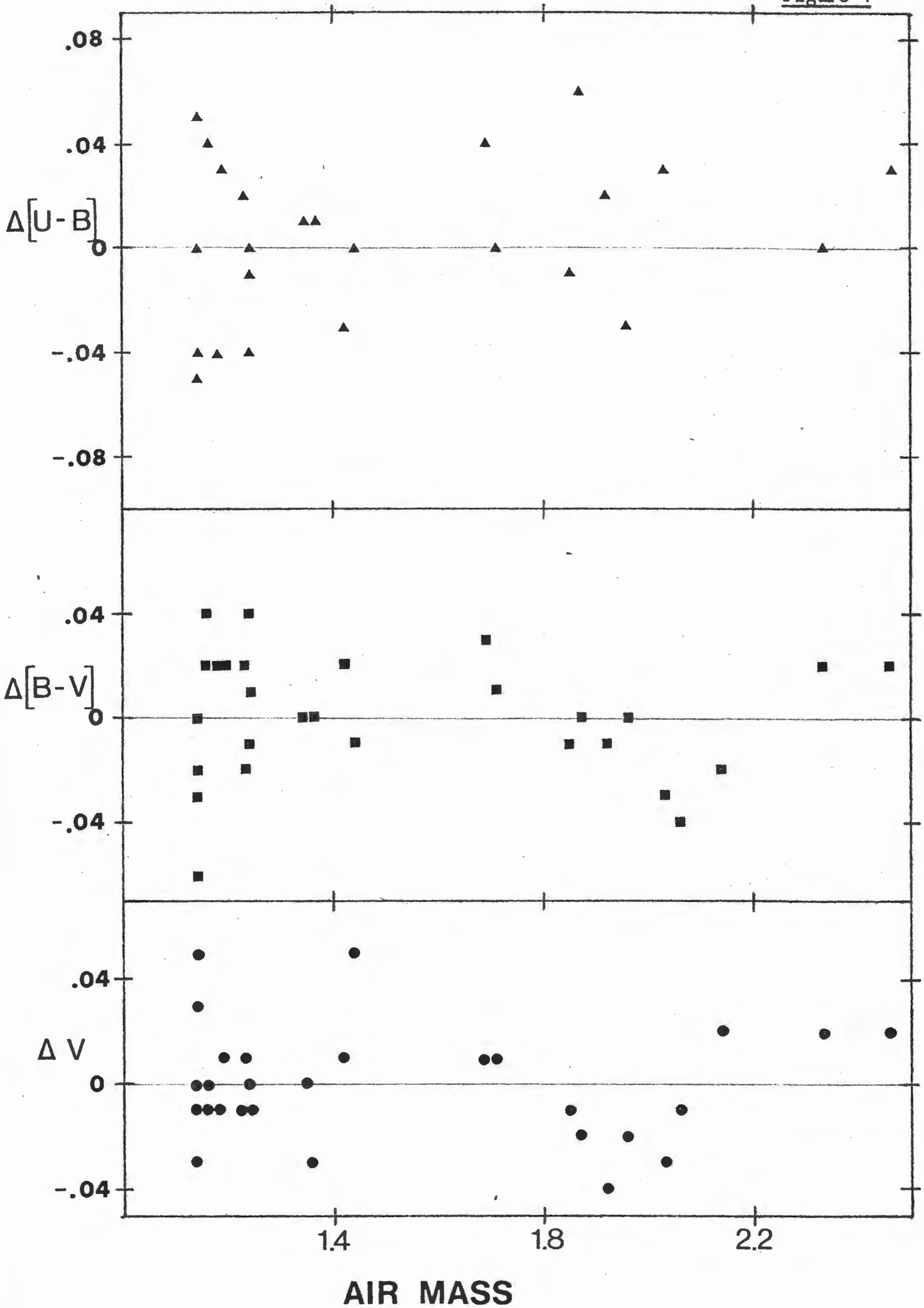

Figure 5

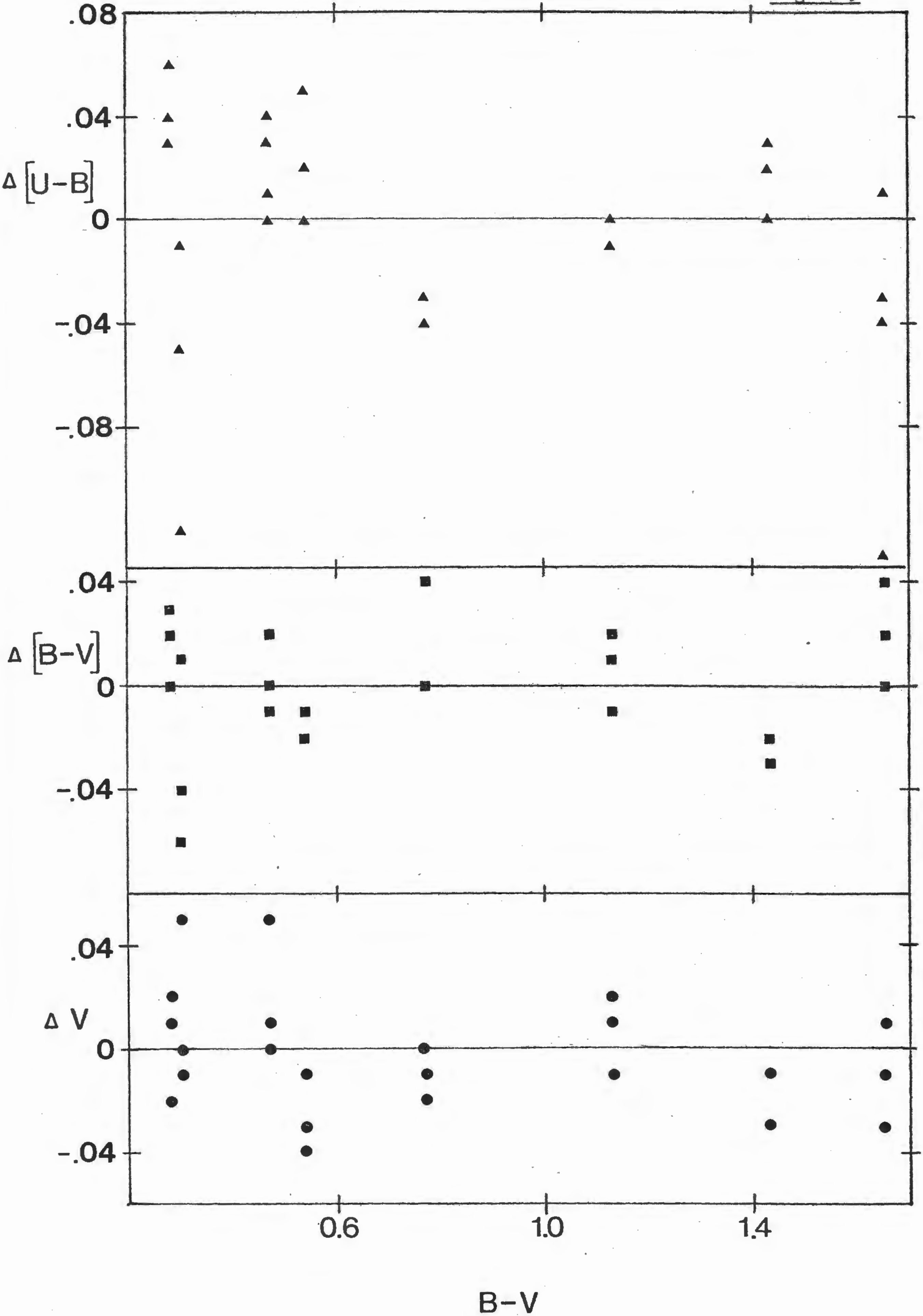

$$V-v_o = 0.053(b-v)_o + 3.337$$

$$B-V = 0.927(b-v)_o + 0.993$$

$$U-B = 1.232(u-b)_o - 0.751$$

$$k_v = 0.131 \pm 0.033$$

$$k'_{bv} = 0.082 \pm 0.008$$

$$k''_{bv} = -0.018 \pm 0.043$$

$$k'_{ub} = 0.274 \pm 0.150$$

with the following r.m.s. errors in the residuals of standard star observations:

$$V = 0.016 \text{ mag}$$

$$(B-V) = 0.023 \text{ mag}$$

$$(U-B) = 0.037 \text{ mag}$$

for a total of five standard star observations.

2.4 Results

The observed photoelectric data for the cluster photoelectric sequence stars were reduced to the UBV system by means of the transformations derived for each night. Most of the cluster photoelectric sequence stars were observed more than once. Table II shows the mean UBV values for all observed cluster photoelectric sequence stars formed by combining the observations of Dr. Welch (1975) with the 1976 observations, the standard deviations from the means, and the number of observations. The magnitudes and colours show good agreement between the various dates of observation; 1975 (Dr. Welch) and 1976.

The mean magnitudes and colours for the cluster photoelectric sequence stars were adopted as standard values to be used in defining the photographic calibration curves.

Mean Magnitudes and Colours of Photoelectric Sequence Stars

TABLE II

	Star	U-B		B-V		V		n
NGC 6604	A	- 0.44	± 0.26	0.75	± 0.03	10.48	± 0.02	5
	B	+ 1.76	0.16	1.90	0.09	12.51	0.05	4
	C	+ 0.83		0.73		15.43		1
	D	- 0.38	0.09	0.70	0.04	12.10	0.05	6
	E	- 0.61	0.04	0.60	0.04	9.19	0.02	2
	G	- 0.31	0.01	0.18	0.01	7.94	0.02	2
	H	- 0.53	0.08	0.60	0.03	10.15	0.05	5
	J	- 0.27	0.11	0.69	0.03	12.21	0.08	4
	K	+ 0.19		0.52		13.82		1
	M	- 0.44	0.04	0.69	0.04	12.16	0.04	2
	N	- 1.14		1.67		13.83		1
	Q	- 0.36		0.84		10.78		1
	S	+ 3.41:		2.26:		13.20		1
	U	- 0.09	0.09	0.76	0.07	13.61	0.05	2
	Y	- 0.50	0.01	0.63	0.01	10.31	0.01	2
	Z	- 0.44	0.01	0.67	0.01	11.58	0.06	2
NGC 6704	A	+ 2.15	± 0.08	2.04	± 0.01	11.35	± 0.04	4
	B	+ 0.65	0.56	1.14	0.11	14.40	0.06	3
	D	+ 0.85	1.53	0.15	0.03	8.65	0.01	4
	F	+ 0.80	0.36	0.83	0.05	13.18	0.05	4
	G	+ 0.35	0.03	0.85	0.04	11.15	0,02	4
	H	+ 0.15	0.34	0.64	0.06	13.24	0.10	4
	J	+ 1.33	0.65	1.84	0.09	14.40	0.03	2
	K	---		2.64		13.66		1

3.) PHOTOGRAPHIC PHOTOMETRY

3.1 Observations

The photographic plates obtained by Dr. Welch in 1975 were taken with the reflecting lens of Racine (1974) in the optical path of the 61-cm telescope, in order to secure secondary images of the brighter stars. These secondary images, approximately 6 magnitudes fainter than the primary images, may, in principle, be used in conjunction with a skeletal photoelectric sequence in the cluster field to determine the photographic calibration of the iris photometer measures. The magnitude difference between the primary and secondary images is dependent on the index of refraction of the lens and any coating on the lens; the 6 magnitude difference is achieved with a SiO overcoat. Unfortunately, it was discovered later that the SiO overcoat had apparently deteriorated, so that the coating across the lens was no longer acceptably uniform. This rendered the secondary images unreliable in defining a photographic calibration curve. Without the secondary images it was necessary to obtain a more complete photoelectric sequence in the cluster field in order to define the calibration curves. It was also desirable to obtain photographic plates taken without the Racine lens to aid in the identification of secondary images on those plates where the Racine lens was used.

Table III gives the plate numbers, exposure times, plate/filter combinations, dates of observation, and comments by the observer on plate quality for the plates taken in June 1975 by Dr. Welch and those taken in 1976. The level of the sky

TABLE III

Plate Information

NGC 6604

plate		exposure	emulsion	filter	date	comment
V	2724	50^m	103a-D	RG 495	13/14-6-75	OK
	2729	50	"	"	14/15-6-75	OK
	2736	50	"	"	15/16-6-75	OK
B	2723	50^m	103a-0	GG 385	13/14-6-75	OK
	2730	50	"	"	14/15-6-75	fuzzy images
	2973	60	"	"	23/24-7-76	OK
U	2740	120^m	103a-0	UG-2	16/17-6-75	seeing not good
	2741	120	"	"	16/17-6-75	OK
	2971	90	"	"	23/24-7-76	OK

NGC 6704

plate		exposure	emulsion	filter	date	comment
V	2718	50^m	103a-D	RG 495	12/13-6-75	OK
	2725	50	"	"	13/14-6-75	seeing not the best
	2742	50	"	"	16/17-6-75	OK
B	2739	50^m	103a-0	GG 385	15/16-6-75	OK
	2977	60	"	"	25/26-7-76	guiding?
	2984	60	"	"	29/30-7-76	OK
U	2731	120^m	103a-0	UG-2	14/15-6-75	clouds?
	2976	90	"	"	25/26-7-76	OK
	2732	120	"	"	14/15-6-75	fuzzy images

background on all 18 plates which were measured was very low and uniform across each plate.

3.2 Star Counts

Counts were made of the stars visible on prints of B plates of each cluster in order to estimate the angular size of the clusters prior to measuring the plates. The cluster fields were divided into quadrants centered on an eye estimate of the cluster centre. The field was further divided into six concentric rings, each ring about 1.25 arc-minutes larger in radius than the preceding one. Counts were made in each quadrant to a limiting magnitude of about B = 15.5. Counts were also made in eight areas of 1 arc-minute square located randomly about the cluster at an average radial distance of 10 arc-minutes (i.e. outside the sixth ring) to estimate the projected density of background stars.

The projected cluster centre was found by plotting the number of stars per square arc-minute in each ring for different quadrants, and adjusting the centre of the quadrants until there was an approximately equal density of stars within the first ring for all quadrants. Figures 6 and 7 illustrate the results of these counts, with both the counts for each quadrant superimposed and the mean count for each ring averaged over the four quadrants. The error bars on the mean counts represent the standard deviation from the mean. The background level is also indicated. An estimate of the cluster radii was then found by noting the radial distance at which the star density within the cluster reached the background density. The estimated radii for the clusters are:

Figures 6 and 7

Projected number density of stars brighter than $B = 15.5$, D_r (stars per square arc-minute), plotted versus radial distance R from cluster centre. Upper portions of figure show radial counts for each quadrant: I = △, II = □, III = ▽, IV = ○. Lower portions show mean projected number density, averaged over all quadrants. Error bars are standard deviation from mean. Dashed line indicates sky background in both upper and lower portions of figures.

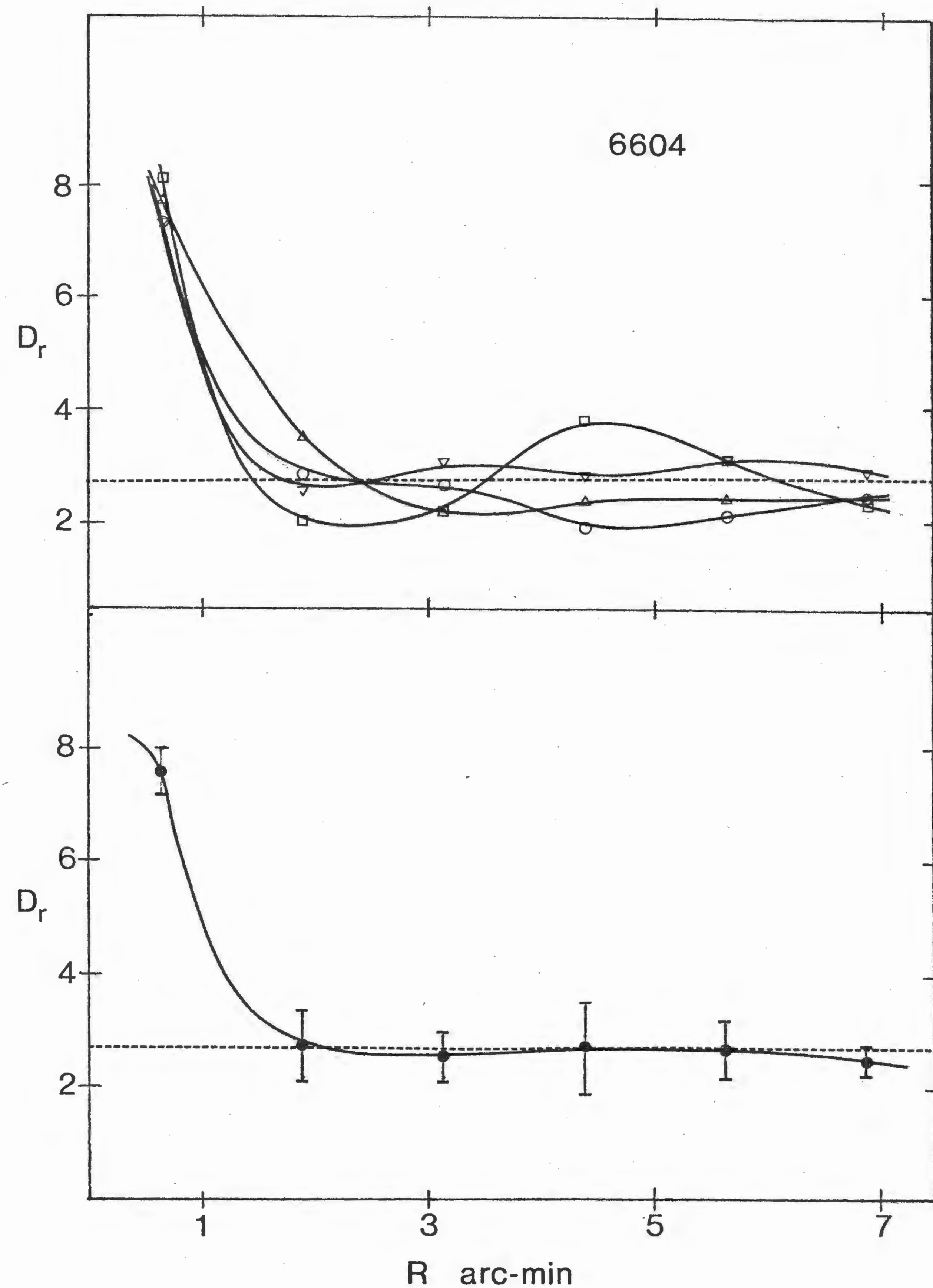
6604
8
6
D_r
4
2
8
6
D_r
4
2
1
3
5
7
R arc-min

Figure 7

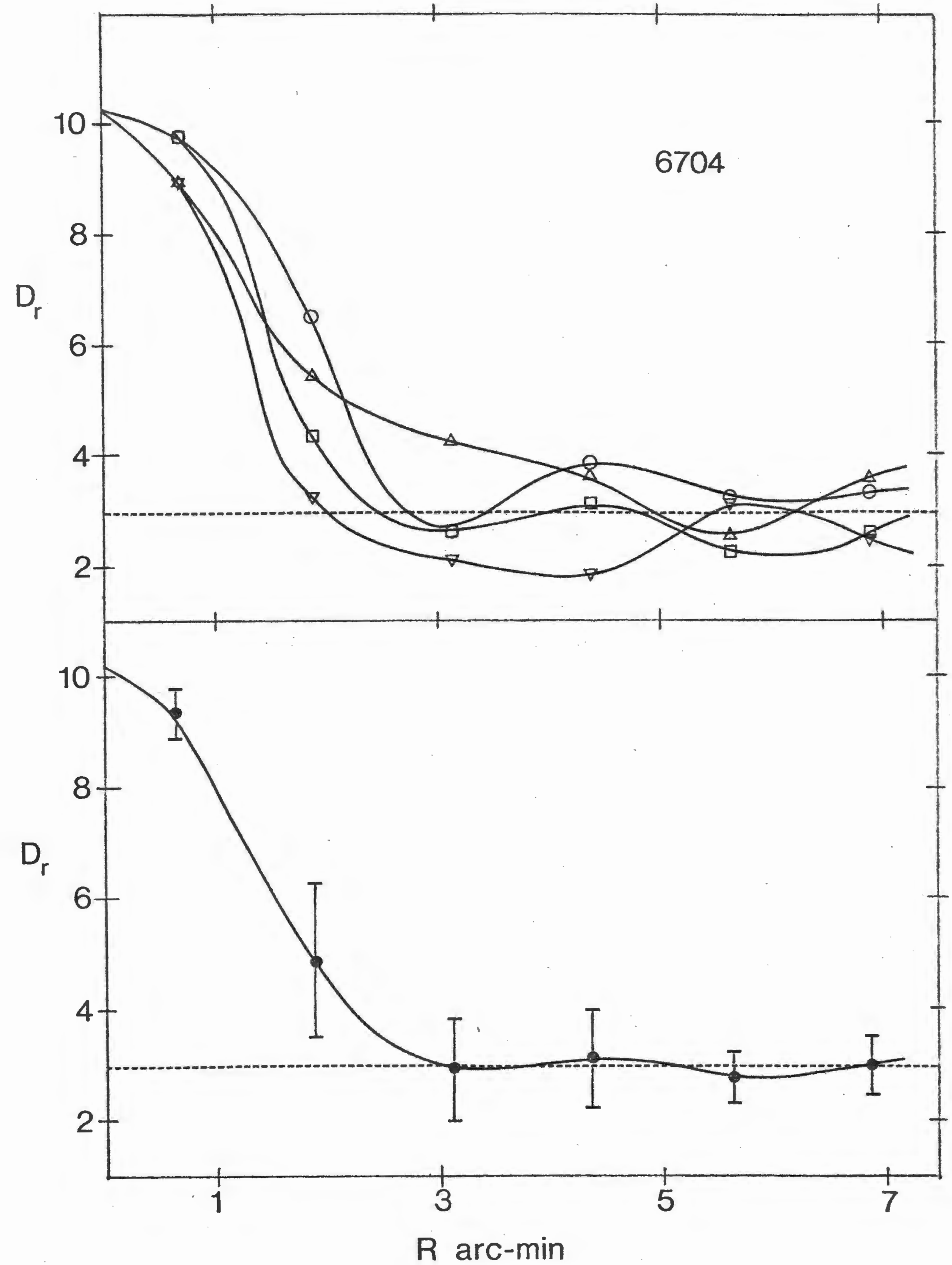

NGC 6604: 2 arc-minutes

NGC 6704 3 arc-minutes

These radii were used to determine a rough limit to the extent of the clusters and to what radial distance stars would be measured. Because of the uncertainty in the estimated radii, all plates were measured out to a radial distance of 5 arc-minutes from the cluster centre. Approximately 100 stars were measured on each plate; the faintest stars (apparent magnitude $V \sim 16$) were well above the plate limit except on the U plates.

3.3 Iris Photometer Problems

Stellar images were measured on an Astro-Mechanics Model A01 iris photometer. Prior to the measurement of the plates, this instrument had been subject to two problems: i) an instability of the null meter used to indicate balance between the comparison and reference beams, and ii) a lack of sensitivity of the null meter to changes in the iris diameter.

Concerning the first difficulty, the field lamp exhibited a rather low cold resistance, causing a heavy surge of current whenever the field lamp was turned on to choose another star for measurement. As wired by Astro-Mechanics, the electronics, the source lamp, and the field lamp were all supplied by one high-quality Lambda power supply. However, the current surge exceeded the capabilities of this 12-volt, 10-ampere power supply; as a result, the voltage on the electronics was reduced almost to zero several times a minute during normal measuring. This problem was solved with the addition of a separate power supply (Lambda model LOS-V-12), isolating the field lamp supply from the original supply for all other 12-volt functions in the photometer.

Concerning the second difficulty, by a lack of "sensitivity" of the null meter, the following is meant. For an iris diameter of 2000 units, a change of 20 units was necessary to produce a change of 10 units on the null meter. This represents a normal sensitivity, or change in the null meter for a given change in the iris size. However, for an iris diameter of 3500 units, a change of 125 units was required to produce a change of 10 units on the null meter. The effect of this is to increase the uncertainty in the iris reading for a null indication on the meter. This problem was never completely solved, in the sense that sensitivity will always be a slight function of iris size, but an acceptable compromise was achieved. By increasing the density of the non-adjustable neutral-density wedge in the reference beam, it was possible to combine a reasonable sensitivity with an iris diameter small enough to allow measurement down to the plate limit.

3.4 Iris Photometer Procedure

Before the actual measurement, each plate was examined for obvious variations of sky fog or development flaws. None were evident on any of the 18 plates. With a plate on the carriage of the photometer and both the iris and plate carefully focused, the iris was positioned on the sky near the plate centre (i.e. near the cluster) and the measurement proceeded as follows:

An arbitrary background iris diameter was chosen as being approximately equal to the size of the faintest image to be measured, yet not so small as to prevent zeroing the null meter by adjusting the wedge. A background iris diameter of ~3500 was common.

Before measuring each star, two background wedge settings were made on either side of a star, about 3-4 stellar diameters away, to exactly zero the null meter at the background iris diameter. This wedge setting was kept constant throughout each measurement, but was readjusted for each star. The star was then centered visually within the iris, and the diameter adjusted to give an approximate null on the meter. The star was then precisely centered by using the carriage controls to minimize the null meter reading. The iris diameter was then adjusted to give exact null. The reading was noted, and the iris diameter then re-adjusted twice more to check on the stability. A mean value of the three iris diameter readings was recorded as the final iris measure. Iris readings were always approached from the same direction to avoid backlash.

During the measuring, the stability proved excellent, while the sensitivity varied only slightly from plate to plate. The readings for a given star were constant to within $\pm$ 1 unit of the iris diameter for the majority of images, and somewhat less (within $\pm$ 5 units) for stars near the plate limit or which had slightly flawed images.

A calibration curve was fitted by eye to the photoelectric and iris photometer data for each plate, using the stars in Table

II for NGC 6604. A typical calibration curve is shown as Figure 8. In the case of NGC 6704, the small number of useable photoelectric sequence stars made it necessary to use those stars measured by Grubbisich (1965) in the RGU photographic system as photoelectric sequence standards. The transformation of RGU colours and magnitudes was made according to the formulae of Steinlin (1968):

$$V = G + 0.05(U-G) - 0.82(G-R) + 0.21 + 0.24E(G-R) - 0.015E^2(G-R)$$

$$B-V = 0.87(G-R) + 0.03(U-G) - 0.32 - 0.17E(G-R) - 0.006E^2(G-R)$$

$$U-B = 0.92(U-G) - 0.05(G-R) - 1.13 - 0.07E(G-R) + 0.02E^2(G-R)$$

It is important to note that there is a potential major source of error introduced by the transformation of the RGU magnitudes and colours because:

1) the magnitudes and colours used to define the calibration curves of Grubbisich were obtained from UBV measures in the cluster M 11 (which was included in the field of Grubbisich's plates) given by Johnson, Sandage, and Wahlquist (1956) and converted to the RGU system, with no quoted errors in the conversion;
2) the RGU values of cluster stars were obtained photographically;
3) the RGU values of cluster stars were then converted to UBV values by the transformations given above.

The iris data and UBV equivalents of the magnitudes and colours of Grubbisich yielded fairly well-defined calibration curves, with the exception of stars that were seen to be visual binaries on the plate, which Grubbisich apparently treated as

Figure 8

A typical calibration curve for NGC 6604. A plot of the iris diameter D_{iris} versus the corresponding V magnitude obtained photoelectrically for cluster sequence stars (solid dots). Open circles represent sequence stars not used to define calibration curve because of misidentification, blended or peculiar image, etc.

Figure 8

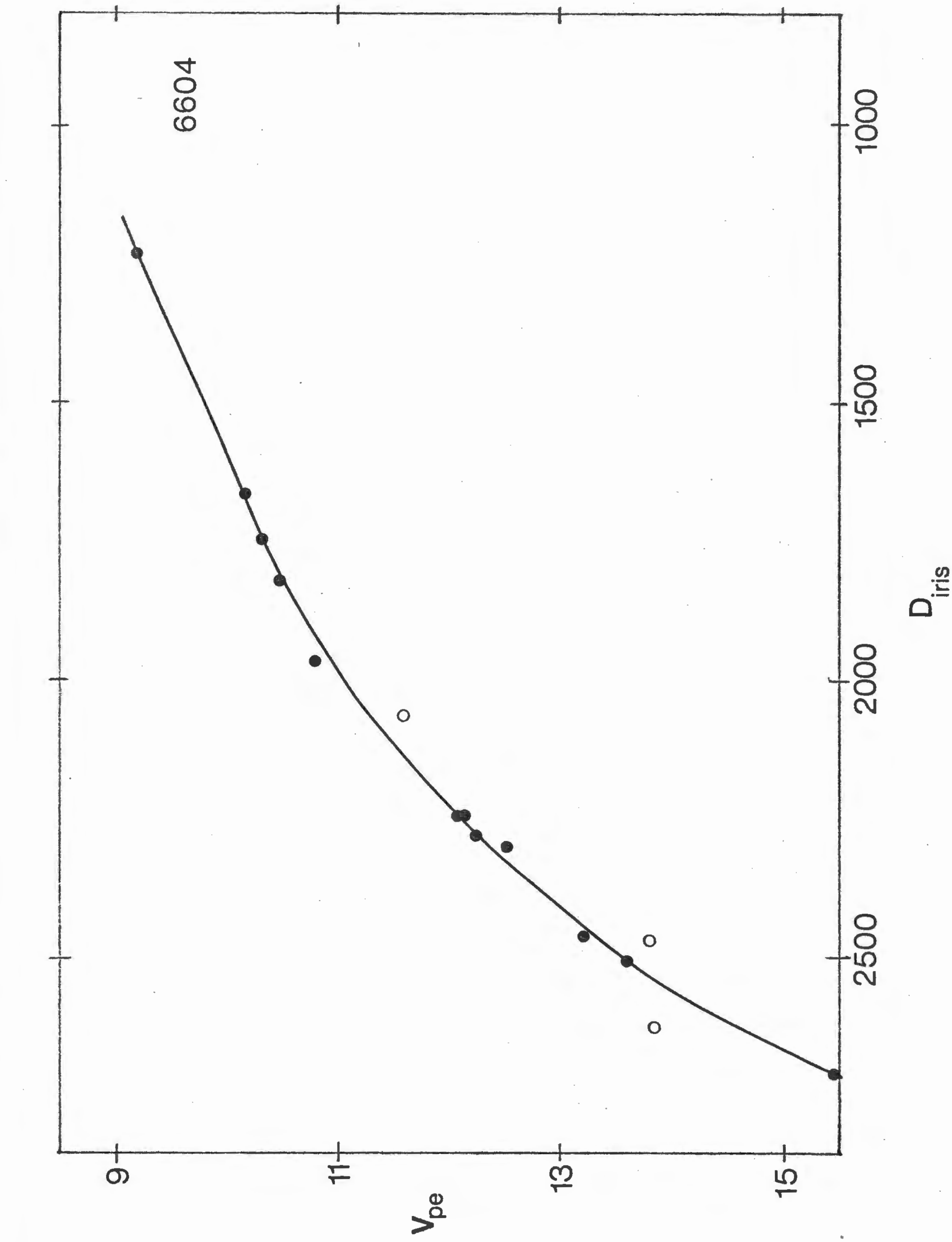

single stars. Those photoelectric values obtained in 1975 and 1976 were also used to help define the calibration curve; there was good agreement between the Grubbisich results and the photoelectric results obtained as part of this study. The magnitudes and colours (in the UBV system) of the Grubbisich stars used in the calibration curves are given in Table IV. Figure 9 shows a typical calibration curve for NGC 6704.

3.5 Results

The photographic values of the photoelectric sequence stars were obtained and plotted versus the instrumental colours to yield transformations to the UBV system, based on linear least squares solutions to these data. The results are:

NGC 6604

$$V-v = 0.001(b-v) + 0.004$$

$$B-V = 0.981(b-v) + 0.027$$

$$U-B = 1.008(u-b) + 0.023$$

NGC 6704

$$V-v = -0.039(b-v) + 0.004$$

$$B-V = 0.927(b-v) + 0.070$$

$$U-B = 1.039(u-b) - 0.023$$

where lower case letter indicate instrumental magnitudes and colours. Residuals, in the sense $\Delta m = m_{pe} - m_{pg}$, were then found and plotted versus colour and magnitude; no significant trends were evident. These plots are given in Figures 10 and 11. The r.m.s. errors of the transformations from the least squares solutions are:

NGC 6604		NGC 6704	
V	= 0.04 mag	V	= 0.04 mag
B-V	= 0.06 mag	B-V	= 0.04 mag
U-B	= 0.09 mag	U-B	= 0.11 mag

The iris measures of the program stars on each plate were then used to obtain instrumental magnitudes from the appropriate calibration curve for that plate. The instrumental magnitudes for all three plates of each colour were then averaged and transformed to the UBV system. Colour indices were formed from the mean magnitudes, i.e. $(B-V) = \langle B \rangle - \langle V \rangle$, $(U-B) = \langle U \rangle - \langle B \rangle$. The standard deviation from the mean of the instrumental magnitudes for each colour was used to check on the consistency of the instrumental magnitudes. In the case of NGC 6604, it was found that plates No. 2973 (B) and No. 2971 (U) gave instrumental magnitudes that differed significantly from the mean of the other two plates in each colour. Both plates in question were taken at large hour angles ($HA \sim 2^h$ east) and may also have been developed somewhat differently than the other plates. Consequently, these two plates were not used to determine mean instrumental magnitudes for NGC 6604.

The UBV data are given in Appendices I and II, along with comments concerning appearance of image (i.e. faint, peculiar, double) and possible cluster membership as determined in the next chapter. The stars are identified by number if observed photographically and by letter if they were photoelectric sequence stars. Finding charts are shown in Plates 1 and 2.

TABLE IV

GRUBBISICH "STANDARD" STARS

Star	U-B	B-V	V
11	0.12	0.57	14.33
16	- 0.11	0.55	12.84
17	+ 0.43	1.09	11.73
21	- 0.14	0.45	13.12
22	+ 0.04	0.55	14.03
23	+ 0.30	0.66	13.99
24	+ 0.10	0.74	14.45
26	- 0.15	0.71	14.78
30	+ 0.76	1.64	12.10
31	+ 0.09	0.55	14.66
32	- 0.06	0.61	15.14
33	+ 0.02	0.76	14.92
34	+ 0.36	0.65	15.25
35	- 0.01	0.91	14.57
37	+ 0.09	0.71	13.94
41	+ 0.15	0.52	14.65
44	+ 0.33	0.67	13.16
47	+ 0.55	0.70	12.98
50	+ 0.04	0.75	14.32

Figure 9

A typical calibration curve for NGC 6704. A plot of the iris diameter D_{iris} versus the corresponding V magnitude transformed from Grubbisich, V_G, for stars used to define the calibration curves (Table IV), shown as solid dots. Open squares are photoelectric sequence stars measured in this study, but not used to define the calibration curves.

Figure 9

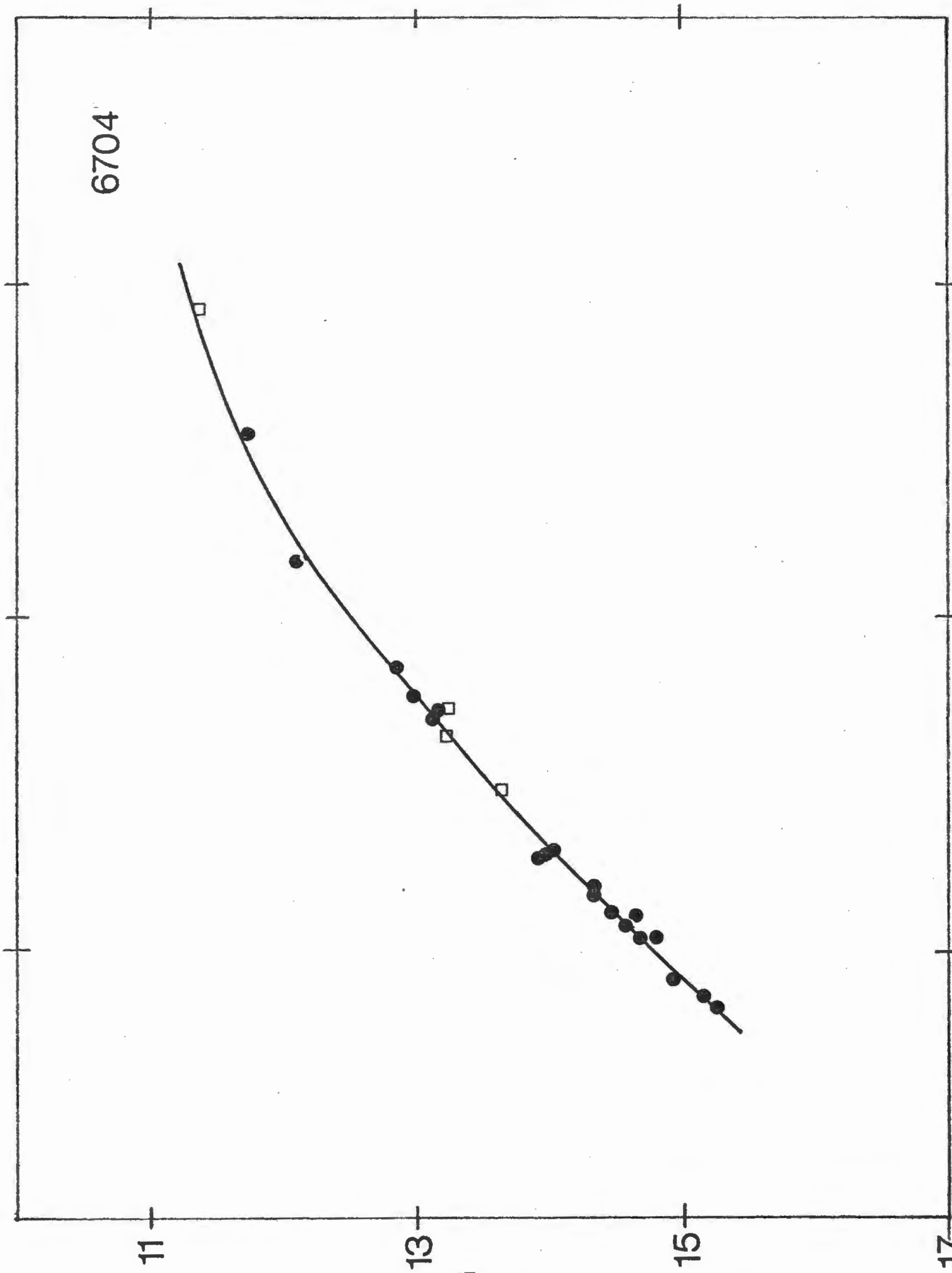

Figures 10a and 10b

Differences between photoelectric and photographic measures, plotted versus magnitude (Figure 10a) and versus colour (Figure 10b) for NGC 6604.

Figure 10a

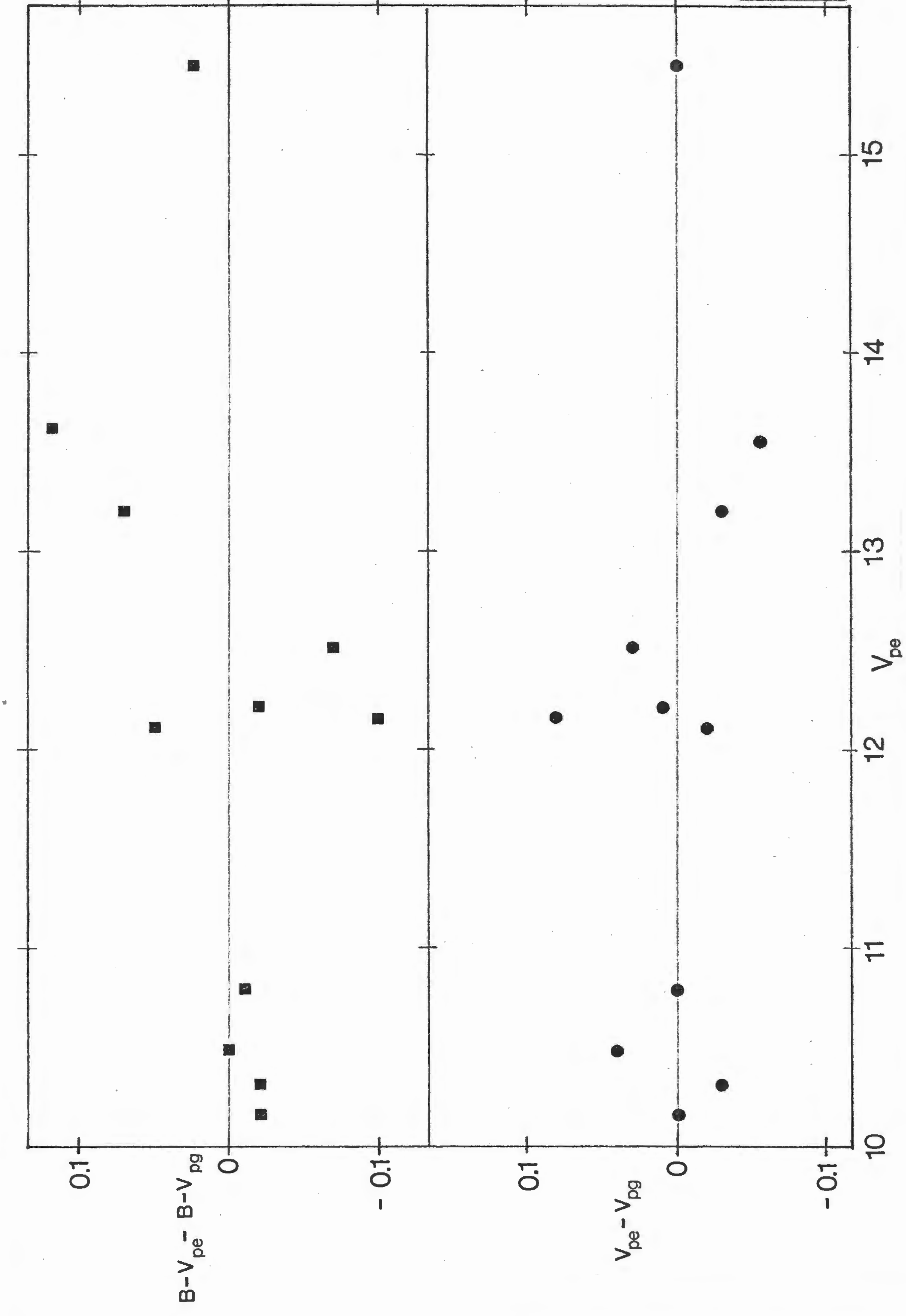

Figure 10b

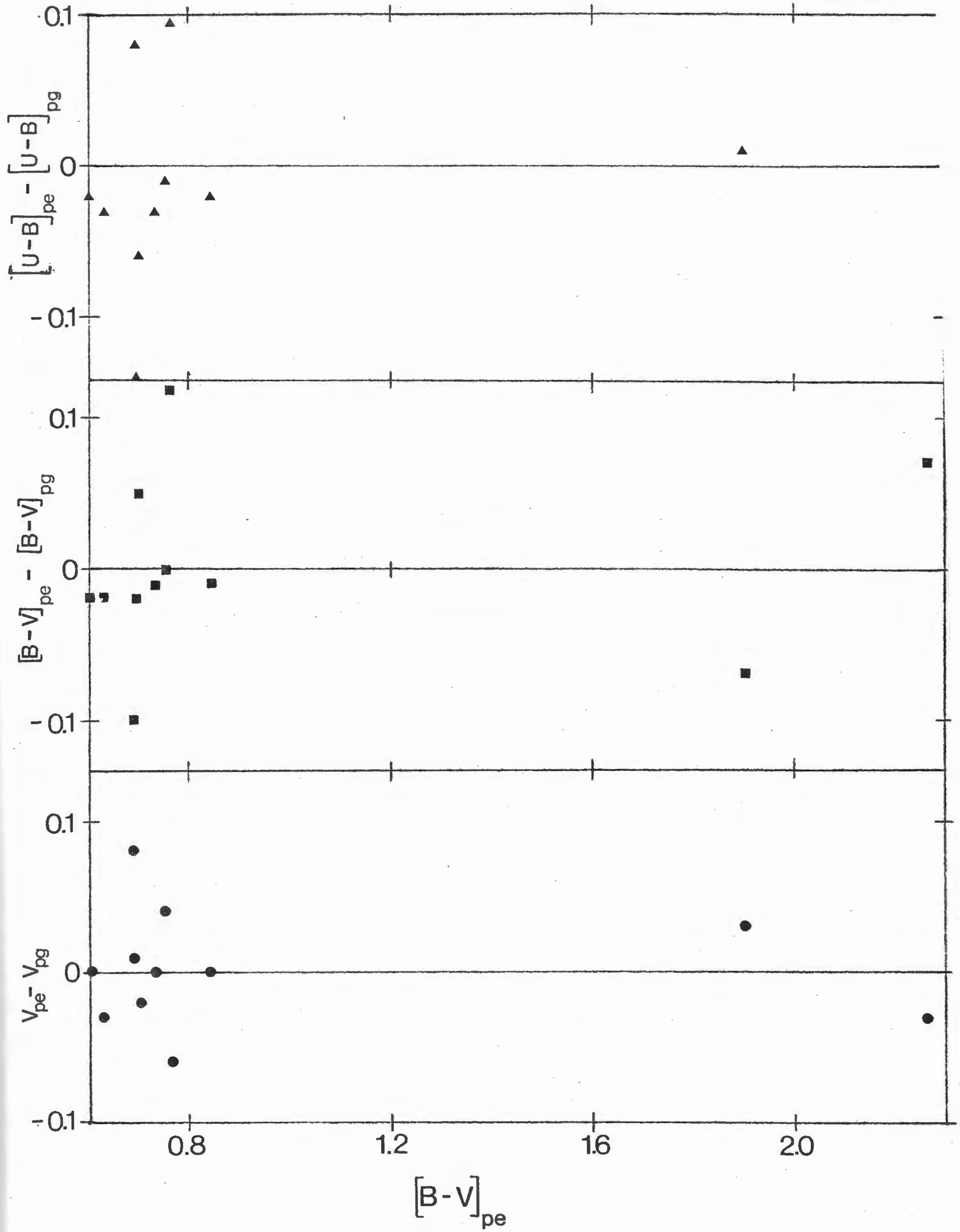

Figures 11a and 11b

Differences between UBV equivalent colours and magnitudes measured by Grubbisich, and photographic measures, in the sense $\Delta m = m_G - m_{pg}$, plotted versus magnitude (Figure 11a) and versus colour (Figure 11b) for NGC 6704.

Figure 11a

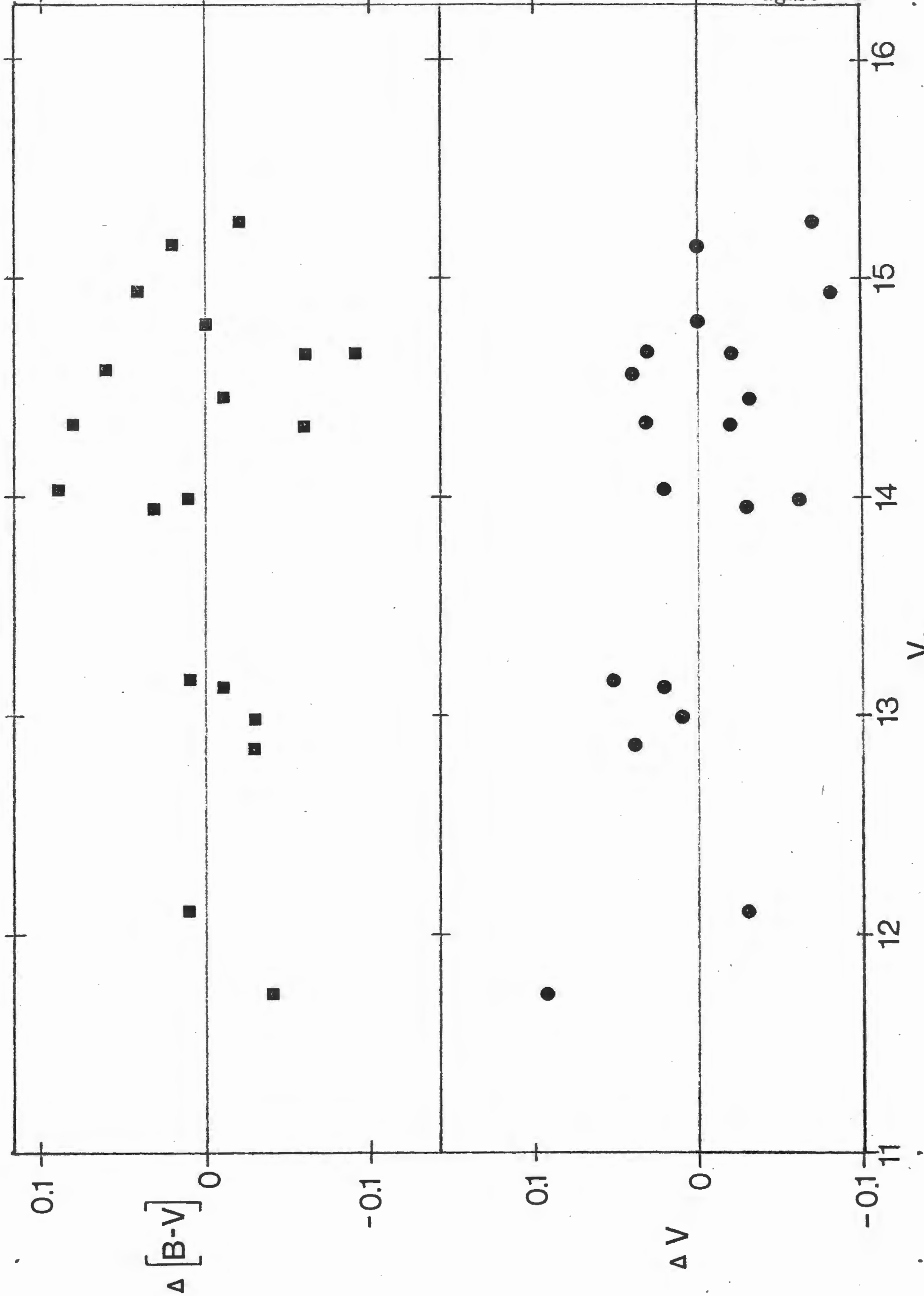

Figure 11b

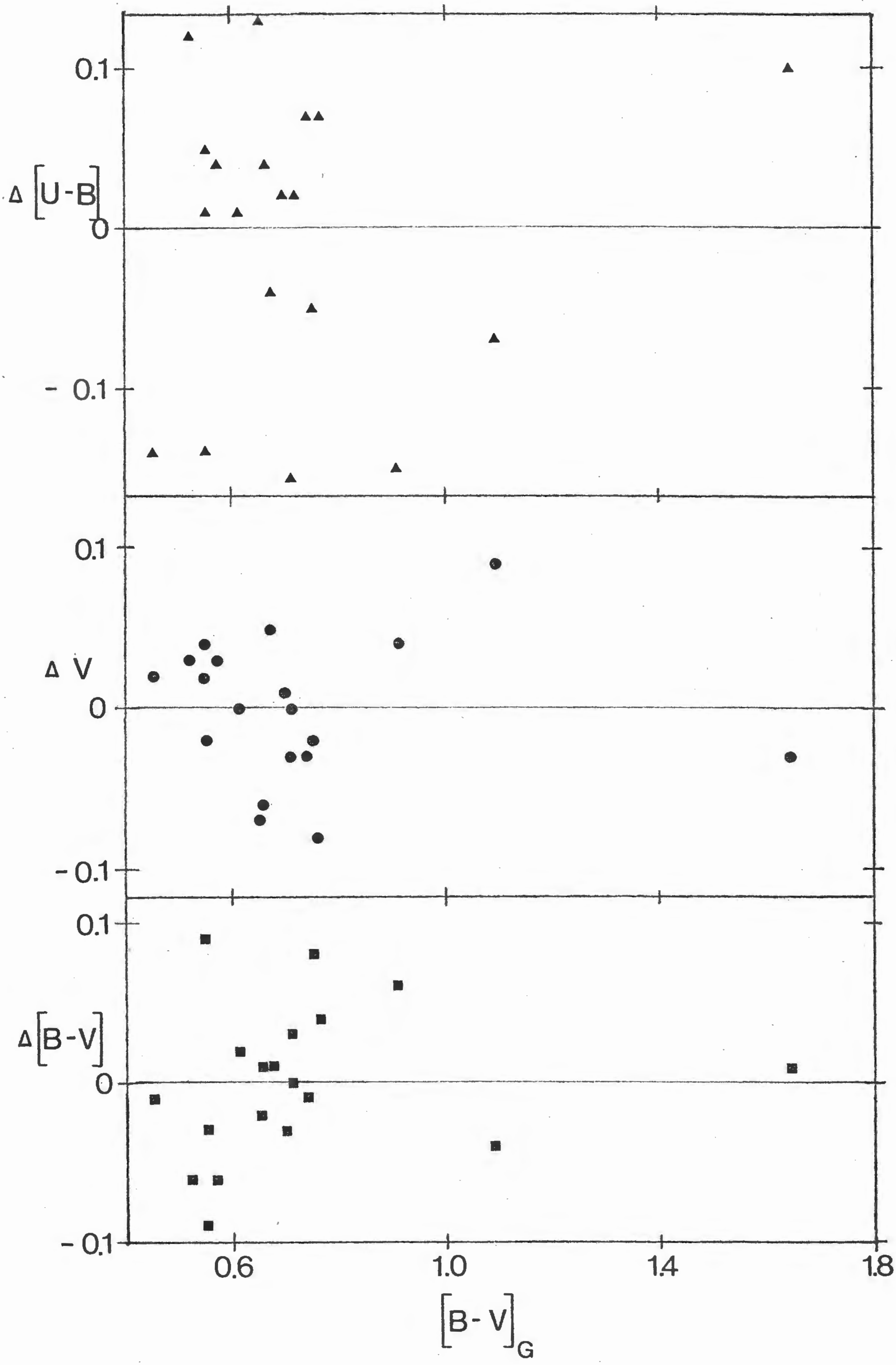

4.) REDDENING AND DISTANCE

4.1 Reddening Corrections

A preliminary estimate of the interstellar reddening was made for each cluster with the "sliding-fit" method (Becker and Stock, 1954) of the two-colour data to the locus of intrinsic colours of main sequence stars (Allen, 1973). The slope of the reddening line was taken as E(U-B) = 0.72 E(B-V). The colour excess estimated in this way was E(B-V) = 0.98 ± 0.05 mag (estimated error) for NGC 6604 and E(B-V) = 0.75 ± 0.05 mag (estimated error) for NGC 6704.

A more comprehensive method to determine interstellar reddening involves the parameter Q (Johnson and Morgan, 1953) defined by:

$$Q = (U-B) - \frac{E(U-B)}{E(B-V)} (B-V) .$$

The parameter Q is independent of interstellar reddening (to a first approximation) and is a measure of the strength of the Balmer discontinuity. The colour excess ratio, E(U-B)/E(B-V), is the slope of the so-called "reddening line" in the two-colour (U-B), (B-V) diagram. For early-type stars, the colour excess ratio is accepted (to first order) as 0.72 ± 0.03 (Allen, 1973). Johnson and Morgan set up an empirical relationship between Q and MK spectral type which is valid for main sequence stars earlier than A0; this relationship therefore provides a method of determining the intrinsic colours $(B-V)_o$ and $(U-B)_o$. Johnson (1958) gives the following relations:

$$(B-V)_o = 0.332\ Q \qquad (B-V)_o = 0.270\ (U-B)_o$$

Becker (1963) illustrates the $(B-V)_o$, Q relationship graphically, and several examples of tables of MK spectral type and corresponding values of Q, $(B-V)_o$, and $(U-B)_o$ can be found in the literature (see for example Golay, 1974). Gutiérrez-Moreno (1975) has reanalyzed the Q-method, finding slight differences between Q and the correponding photometric spectral type S_q as given by Johnson; these differences are not significant in relation to the probable errors of observation in this study, however.

The UBV colour indices in Appendices I and II were employed to compute the intrinsic colour indices for individual stars from the relations of Johnson given above. Individual colour excesses in both (B-V) and (U-B) were calculated using the equations:

$$E(B-V) = (B-V) - (B-V)_o$$

$$E(U-B) = (U-B) - (U-B)_o$$

A mean colour excess $\bar{E}(B-V)$ was found from those cluster photoelectric sequence stars whose calculated colour excess was similar to that given by the sliding-fit; for NGC 6604, seven photoelectric sequence stars were used; for NGC 6704, those stars measured by Grubbisich (1965) which defined the UBV calibration curves were employed. The resulting mean values were:

NGC 6604	$\bar{E}(B-V) = 0.96 \pm 0.02$	$\bar{E}(U-B) = 0.69 \pm 0.02$	(s.d.)
NGC 6704	$\bar{E}(B-V) = 0.71 \pm 0.06$	$\bar{E}(U-B) = 0.51 \pm 0.06$	(s.d.)

MK spectral types were found for only two stars in NGC 6604, although six stars are classified as OB in the <u>Catalogue of Luminous Stars in the Southern Milky Way</u> (Stephenson and Sanduleak, 1970); no spectral types could be found for stars in NGC 6704. The MK spectral type of star E (BD -12° 4982) in NGC 6604 is B0 (Morgan, Whitford, and Code, 1953), yielding a colour excess of E(B-V) = 0.96 (Miller, 1968), in accord with the mean value given above. Moffat and Vogt (1975) derived E(B-V) = 1.01 for NGC 6604, based on UBV photometry of seven bright cluster stars.

The visual absorption is given by $A_v = R \cdot \bar{E}(B-V)$, where R is the ratio of total to selective absorption. The standard value of R has generally been 3.0 ± 0.2 (Hiltner and Johnson, 1956); recent work has yielded a new value, now generally accepted, of $R = 3.3 \pm 0.2$ (Sandage, 1975; Crawford, 1976; Herbst, 1975). The more recent result is adopted here, to give:

NGC 6604: $A_v = 3.17 \pm 0.20$ mag NGC 6704: $A_v = 2.34 \pm 0.21$ mag

Figures 12, 13, 14, and 15 show the UBV data from Appendices I and II plotted on the two-colour diagram (TCD) and colour-magnitude diagram (CMD) with main sequence loci shifted to agree with the adopted values of reddening and absorption. The shape of the zero-age main-sequence (ZAMS) was taken from Blaauw (1963), but all stars were made more luminous by 0.18 mag to correspond to the change in the distance modulus of the Hyades cluster as suggested by van Altena (1974). This

Figures 12 and 13

Figure 12: Two-colour diagram (TCD) for NGC 6604. A plot of observed (U-B) versus (B-V) colours. The solid line is the locus of intrinsic colours of main sequence stars corrected for reddening of E(B-V) = 0.96 and E(U-B) = 0.69. Solid dots are stars which are probable cluster members (see section 4.2), open circles are probable non-members. Open squares are cluster members observed by Moffat and Vogt but not in this study, solid square is HD 167971, the central star of the cluster.

Figure 13: Colour-magnitude diagram (CMD) for NGC 6604. A plot of observed V, B-V values. Symbols are the same as in Figure 12.

Figure 12

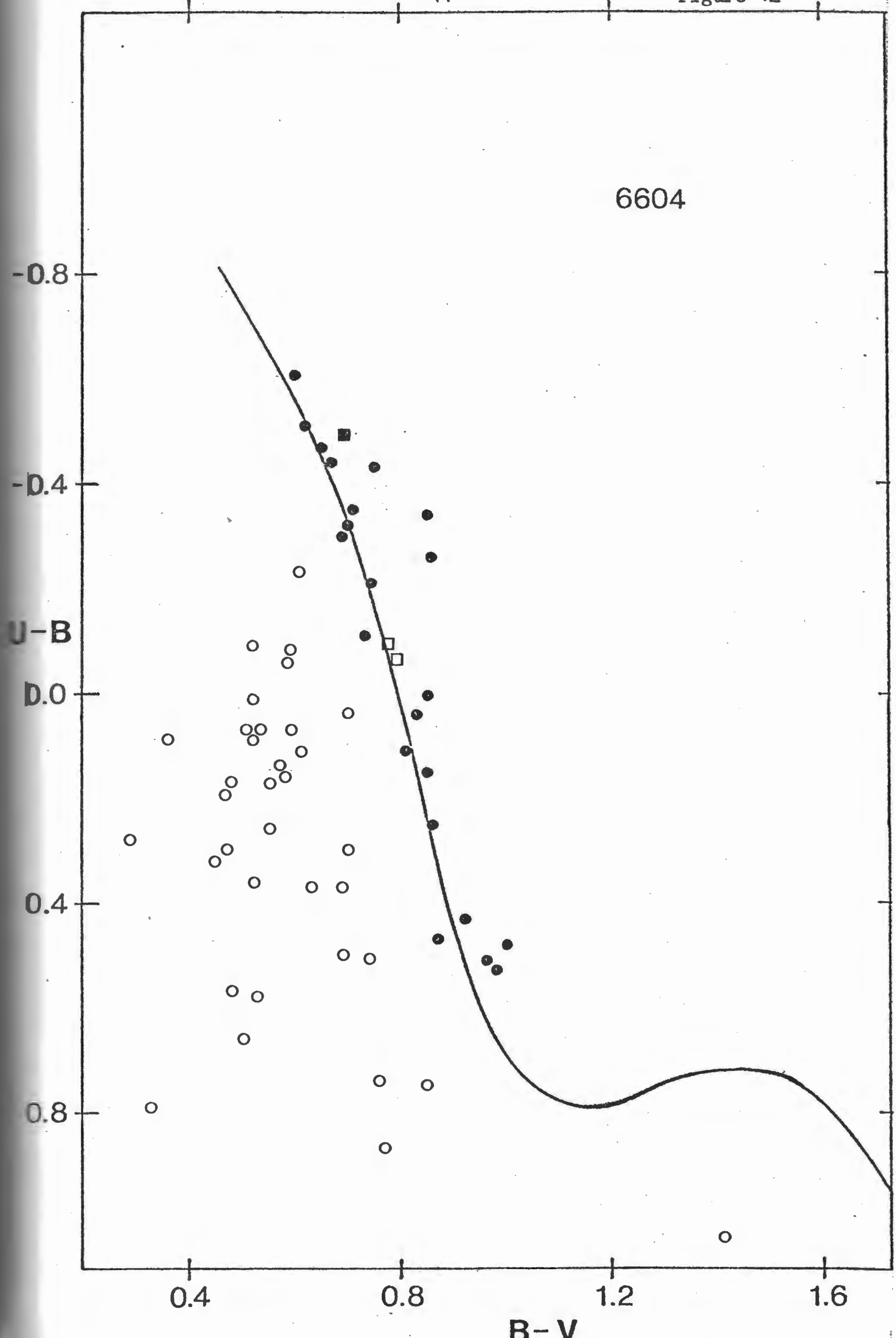

Figure 13

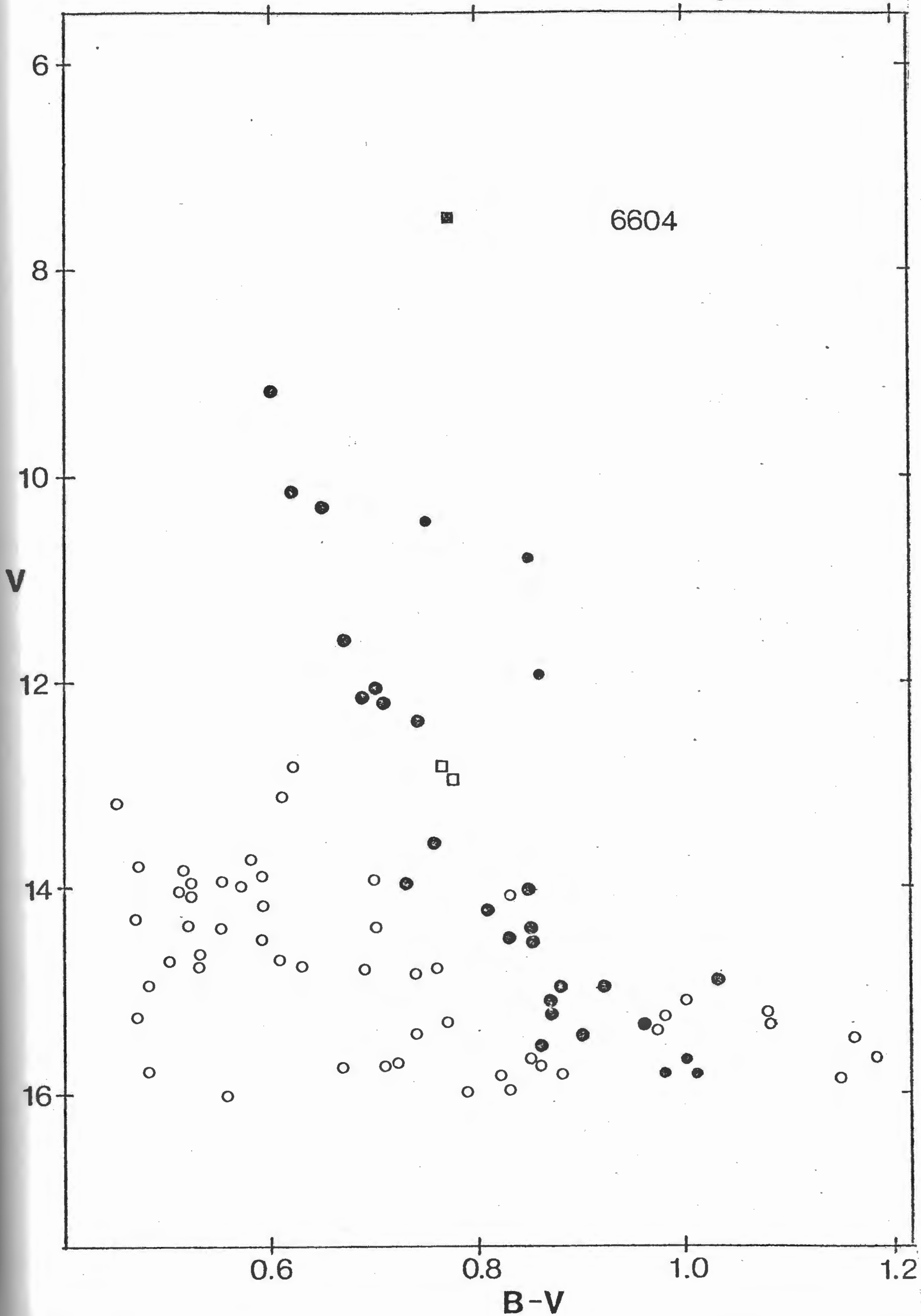

Figures 14 and 15

Figure 14: Two-colour diagram (TCD) for NGC 6704. Solid symbols are probable members; triangles are visual binaries, square is star FN Sct. Open circles are probable non-members (see section 4.2). Solid line is locus of intrinsic colours of main sequence stars corrected for reddening of E(B-V) = 0.71 and E(U-B) = 0.51.

Figure 15: Colour-magnitude diagram for NGC 6704. Symbols are the same as in Figure 14.

Figure 14

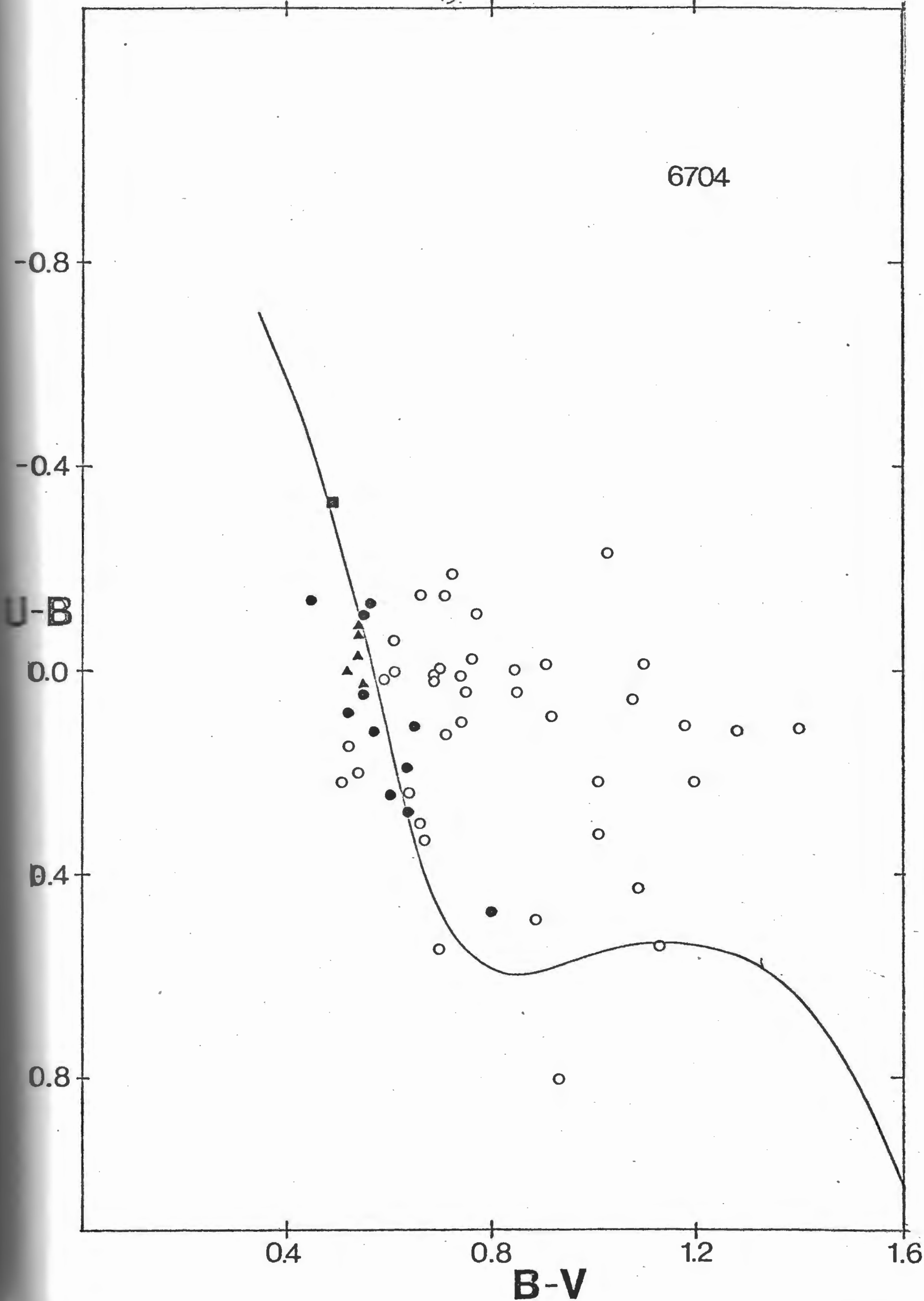

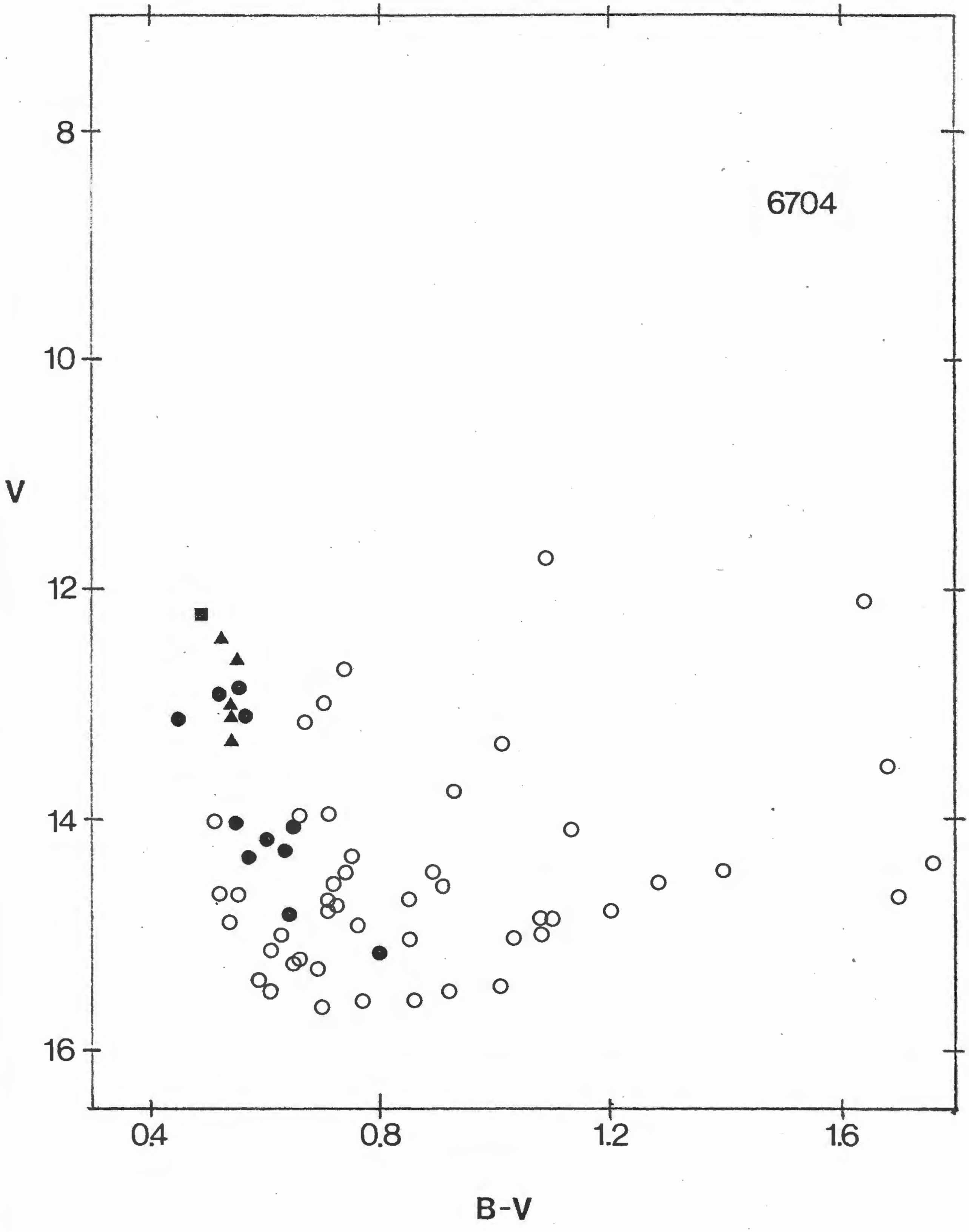
6704
V
8
10
12
14
16
0.4
0.8
1.2
1.6
B-V

revised ZAMS will be used throughout the remainder of this study.

For NGC 6604, stars 91, A, and Q have different (i.e. larger) reddening than the rest of the cluster members and are all seen to one side of the cluster. They were therefore un-reddened differentially to the mean of the other members on the CMD. These stars were not used in the determination of distance modulus.

Figures 16 and 17 illustrate the variation of reddening across each cluster. For NGC 6704, the variation seems to be random; for NGC 6604, the overall extinction appears to increase from northeast to southwest, with a suggestion of a band of higher reddening (dust lane?) trending northwest-southeast at a radial distance of about 2.5 arc-minutes from the cluster centre.

4.2 Cluster Membership and Distance Moduli

An examination of values of colour excess E(B-V) and location on the TCD and CMD led to the elimination of obvious non-members of the two clusters. The absolute visual magnitudes M_V of the remaining stars were then determined from the intrinsic $(B-V)_0$ colours and the ZAMS. The apparent visual magnitudes V were corrected for absorption using the equation $V_0 = V - A_V$.

Following the example of Walker (1965), cluster membership was investigated by means of a (V_0, M_V) diagram. Figures 18 and 19 show such a diagram for each cluster. Stars within the strip defined by the dashed lines are considered to be members. These defining limits are set by assuming that no cluster member will

Figures 16 and 17

Variation of colour excess E(B-V) across NGC 6604 (Figure 16) and across NGC 6704 (Figure 17). Solid dots represent positions of cluster members. Numbers are values of E(B-V) with decimal point omitted (i.e. 97 = 0.97, 101 = 1.01, etc.). Scale is indicated by tick marks at radial distances of 5 arc-minutes. In Figure 16, stars identified by letter (Q,A) or number (91) are stars which were de-reddened differentially (see text).

Figure 16

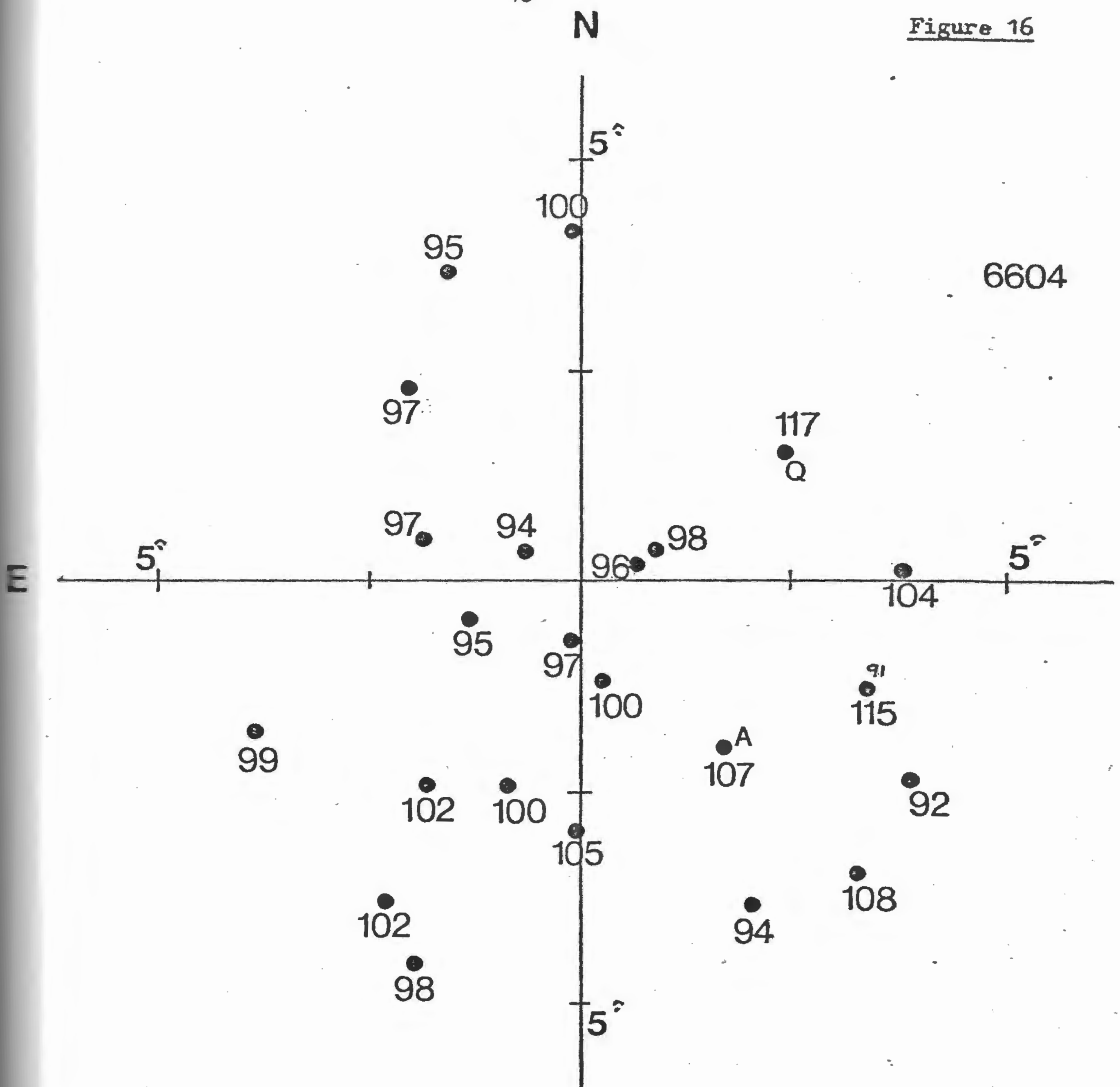
N
E
5°
5°
5°
5°
6604
100
95
97
117
Q
97
94
98
96
104
95
97
100
91
115
A
107
99
102
100
92
105
108
102
94
98

Figure 17

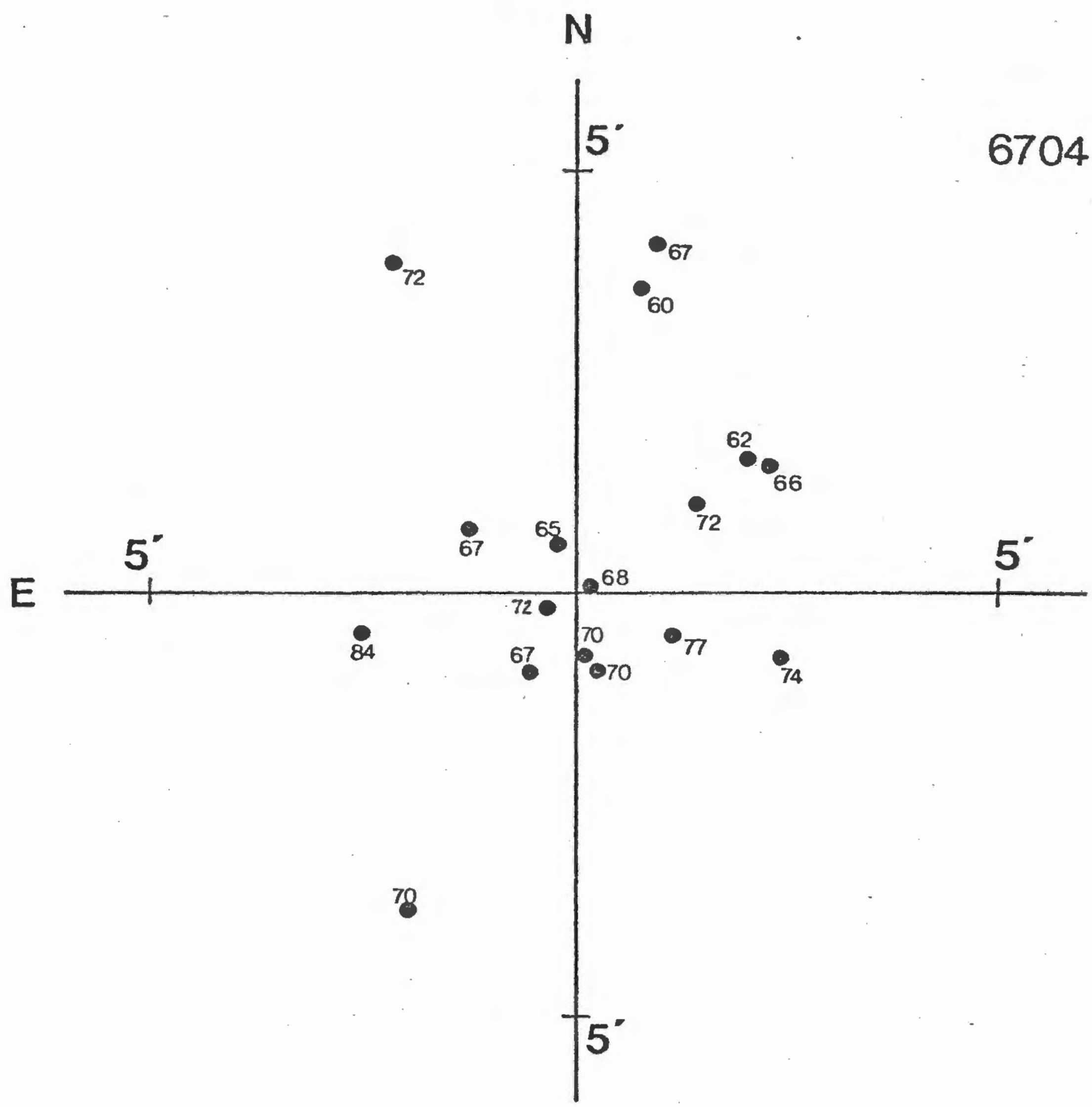

lie more than 0.5 mag above the line $V_o = M_v$ + constant and that duplicity will not brighten a star by more than 0.75 mag. The brightest members may lie outside the strip if they are in the process of evolving away from the main sequence. The constant in the expression $V_o = M_v$ + constant is the cluster distance modulus, determined from both a sliding fit of the observed CMD to the ZAMS and from a mean value of $(V_o - M_v)$ formed from those stars used previously in determining the colour excesses. A mean distance modulus was later recalculated using only those stars which lie within the membership envelope on the (V_o, M_v) diagram.

The evolutionary deviation curve of Johnson (1960) was also used to estimate the distance modulus. The method involves the sliding fit of an empirically-derived curve (whose shape is fixed by data given by Johnson) to a plot of $(V_o - M_v)$ versus V_o for cluster members. The curve represents the mean deviation from the main sequence of stars in clusters with a relatively wide spread in age. That value of $(V_o - M_v)$ which is approached asymptotically by the faint (right-hand) portion of the curve, as seen in Figures 20 and 21, is the cluster distance modulus.

The distance moduli obtained in this manner are in good agreement with the mean values calculated above. The adopted distance moduli and corresponding distances are:

NGC 6604: $\overline{V_o - M_v} = 11.62 \pm 0.41$ mag $\qquad r = 2.11 \pm 0.40$ kpc

NGC 6704: $\overline{V_o - M_v} = 11.45 \pm 0.25$ mag $\qquad r = 1.95 \pm 0.23$ kpc

Figures 18 and 19

The V_o, M_v diagrams for NGC 6604 (Figure 18) and NGC 6704 (Figure 19). See text (p. 45) for explanation. Symbols in Figure 19 are the same as in Figure 14.

Figure 18

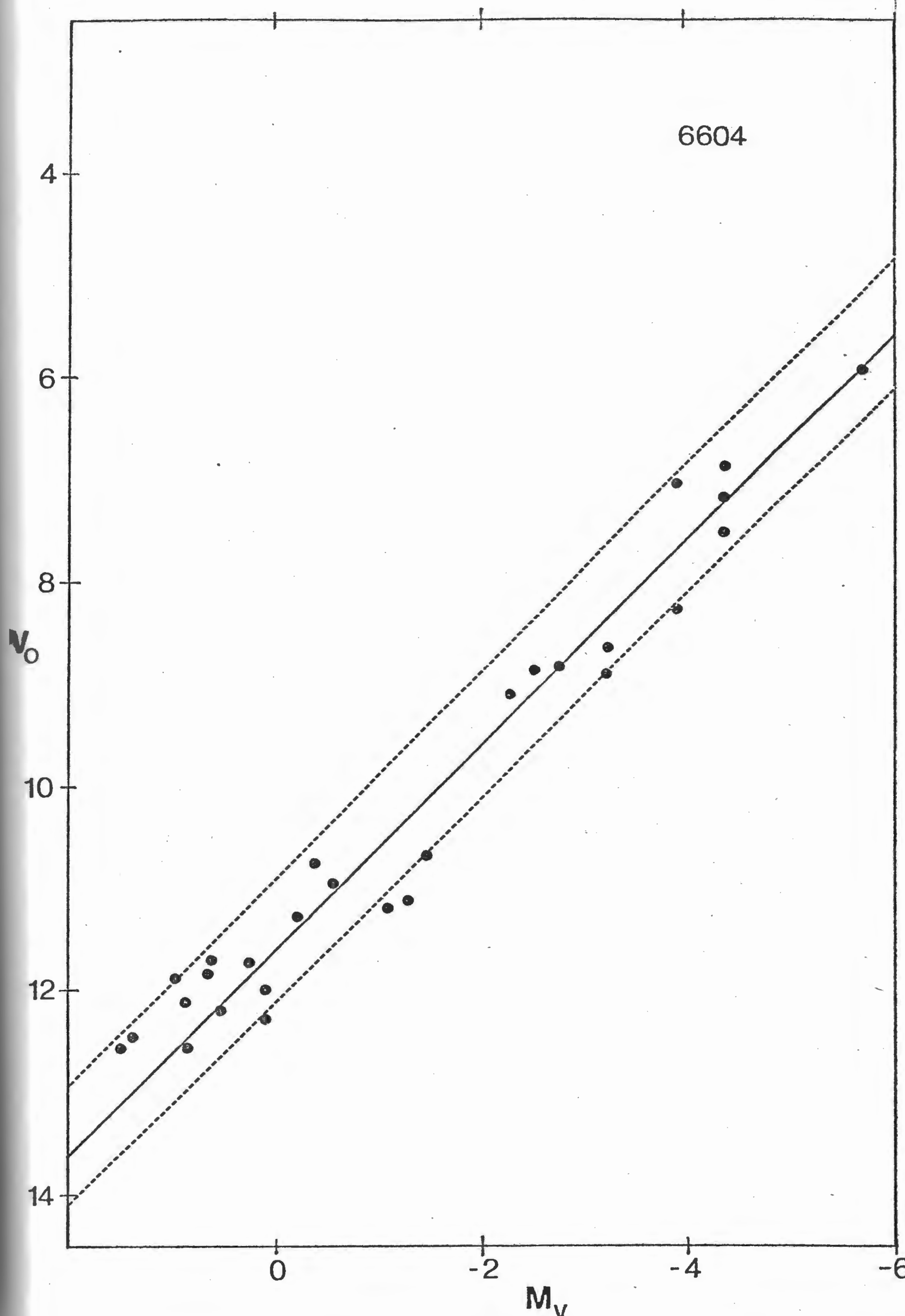

Figure 19

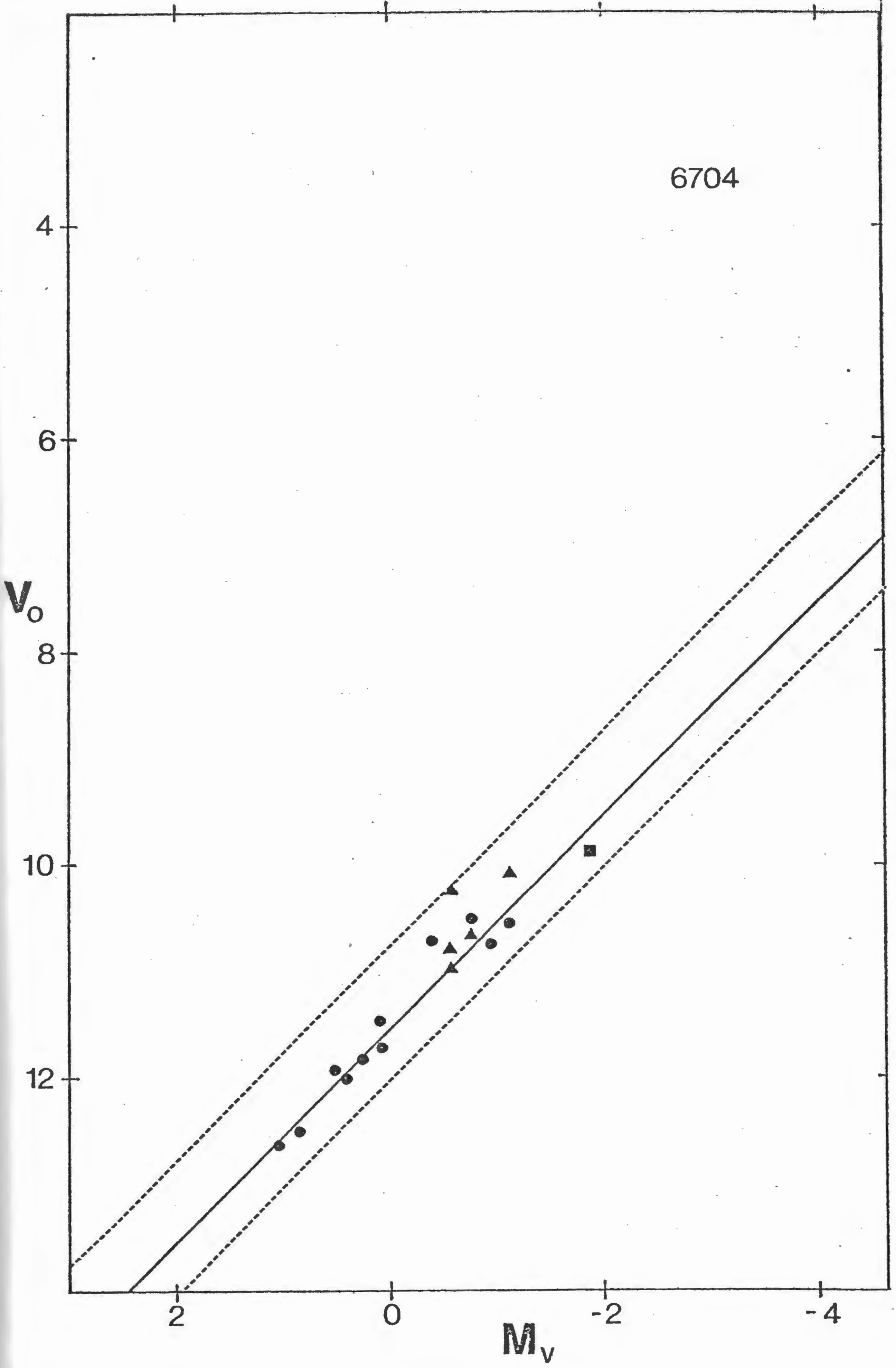

Figures 20 and 21

Evolutionary deviation curves for NGC 6604 (Figure 20) and NGC 6704 (Figure 21). V_o is the apparent visual magnitude corrected for interstellar absorption, and M_v is the absolute magnitude a star would have if it were on the ZAMS. The shape of the curve is fixed and is adjusted for best fit to the data points by motion in both coordinates. The cluster distance modulus is that value of (V_o-M_v) which is approached asymptotically by the right-hand part of the curve.

Symbols in Figure 20: solid dots are photoelectric measures, open circles are photographic measures.

Symbols in Figure 21 are the same as in Figure 14: triangles are visual binaries, solid square is the star FN Sct, solid dots are other cluster members.

Figure 20

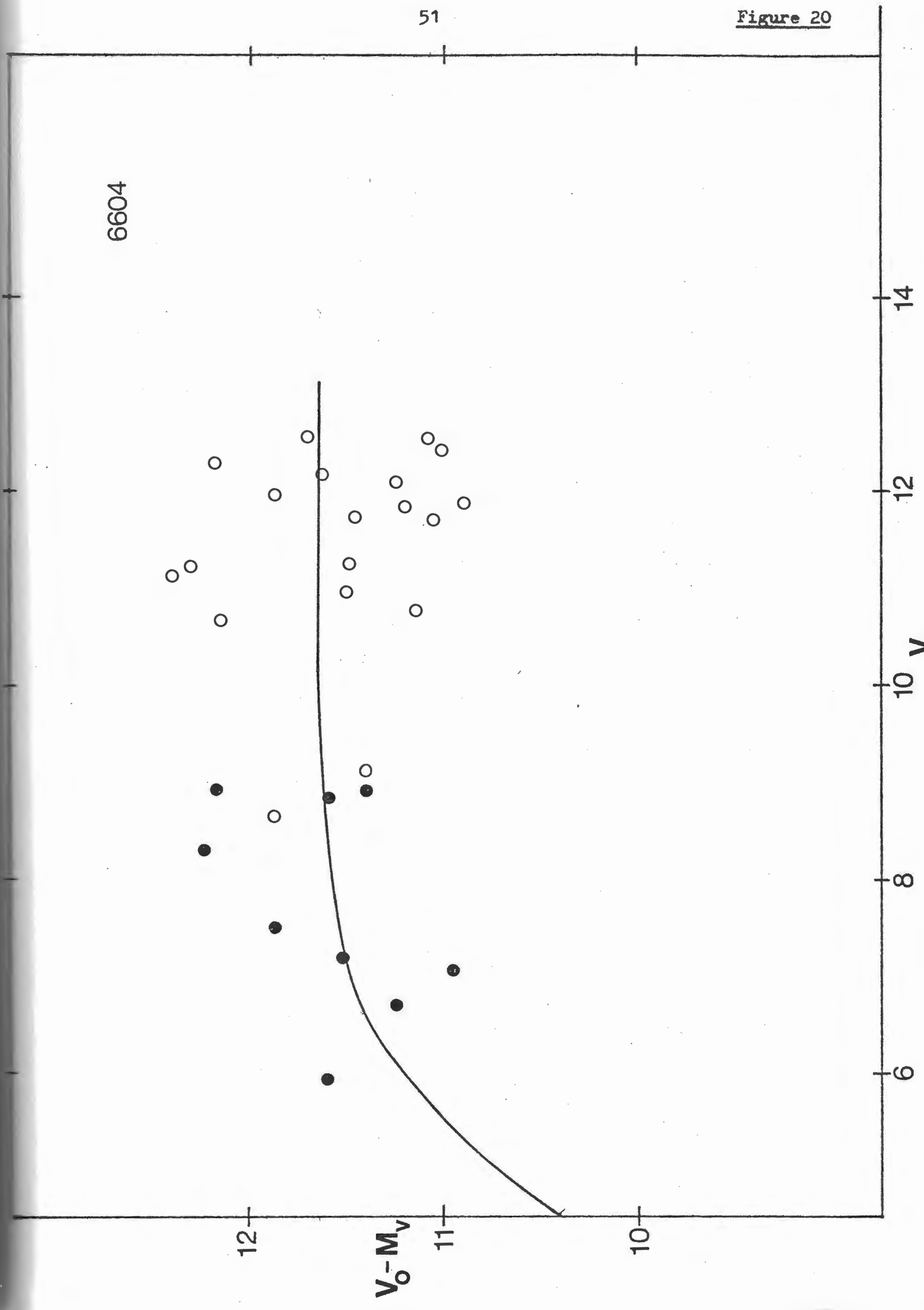

Figure 21

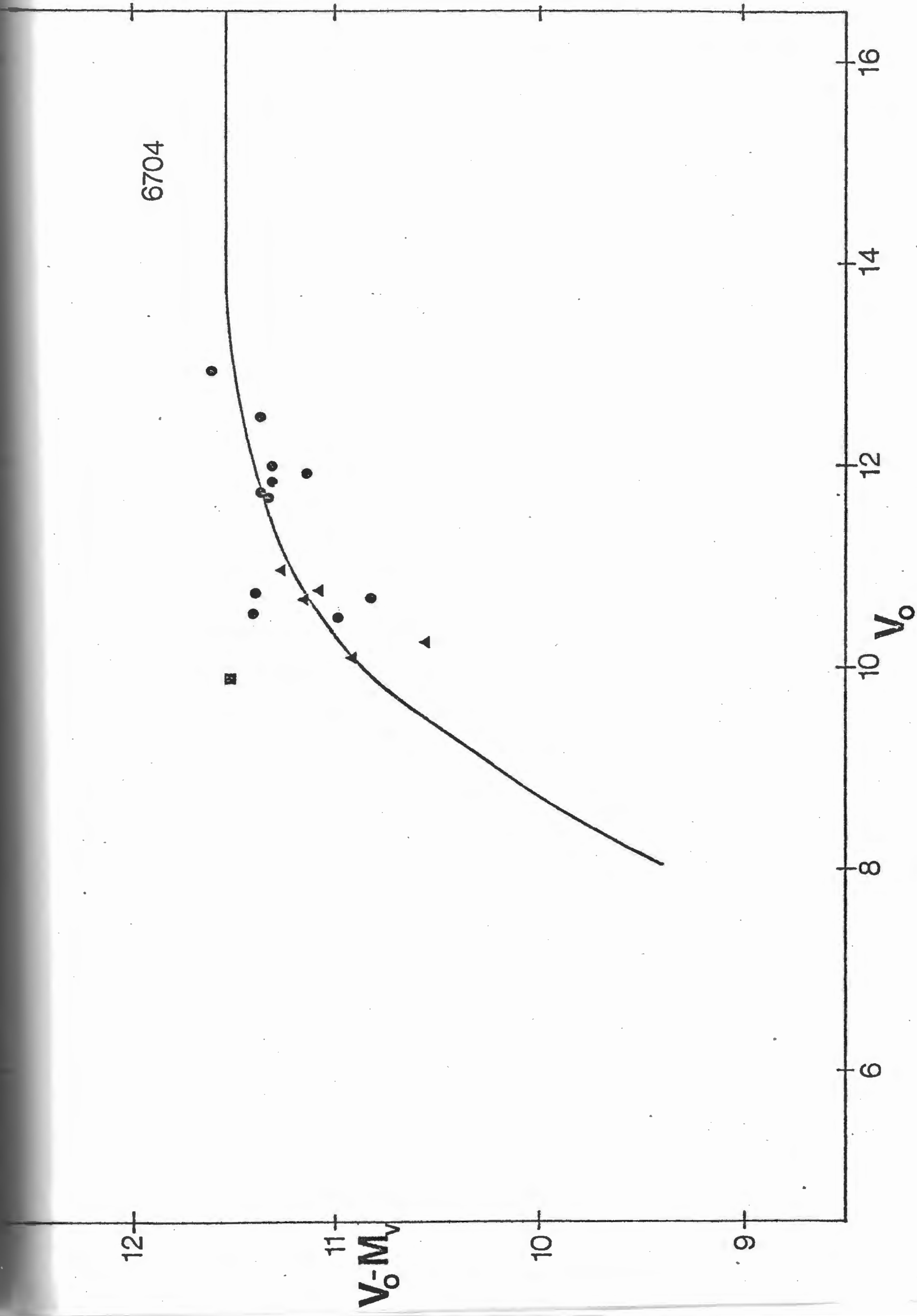

Tables V and VI give UBV magnitudes and colours, colour excesses E(B-V), intrinsic colours $(B-V)_o$, absolute magnitudes M_V, and distance moduli for individual cluster members. For those star in NGC 6604 with no value of E(B-V) given (i.e. those stars with $(B-V)_o \geqslant 0$), the intrinsic colours were found using the mean value of colour excess E(B-V) = 0.96.

It should be emphasized that, without proper motion data or spectral types, the membership of a given star in either cluster should only be considered preliminary (Walker, 1959).

In Figures 22 and 23 are shown the colour-magnitude diagrams for both clusters with probable members only plotted. The zero-age main-sequence has been corrected for the adopted values of reddening, absorption, and distance modulus. The colour-magnitude diagrams are discussed in some detail in the next chapter.

TABLE V

CLUSTER MEMBERS NGC 6604

Star	U-B	B-V	V	E(B-V)	$(B-V)_o$	M_v	V_o-M_v
21	0.53	0.98	15.83	1.04	- 0.06	0.86	11.70
29	1.13:	0.88	14.99	-	- 0.11	0.26	11.46
40	0.43	0.92	14.97	1.00	- 0.08	0.64	11.06
46	0.75:	0.85	14.53	-	- 0.14	- 0.22	11.48
50	0.11	0.81	14.21	0.97	- 0.16	- 0.56	11.50
56	0.04	0.83	14.48	1.02	- 0.19	- 1.10	12.31
58	0.15	0.85	14.03	1.00	- 0.15	- 0.38	11.14
61	- 0.21	0.74	12.38	0.99	- 0.25	- 2.28	11.39
65	-	1.01	15.82	-	+ 0.02	1.47	11.08
66	0.51	0.96	15.36	1.02	- 0.06	0.86	11.23
69	0.25	0.86	15.55	0.98	- 0.12	0.10	12.18
73	-	0.90	15.43	-	- 0.09	0.53	11.63
74	-	0.87	15.24	-	- 0.12	0.10	11.87
79	-	1.00	15.68	-	+ 0.01	1.40	11.01
80	0.00	0.85	14.39	1.05	- 0.20	- 1.28	12.40
87	- 0.11	0.73	13.94	0.94	- 0.21	- 1.48	12.15
89	0.48	1.00	15.10	1.08	- 0.08	0.64	11.19
90	0.47	0.87	15.14	0.92	- 0.05	0.97	10.90
91	- 0.26	0.86	11.96	1.15	- 0.29	- 3.24	11.88
A	- 0.43	0.75	10.44	1.07	- 0.32	- 4.36	11.53
D	- 0.32	0.70	12.10	0.97	- 0.27	- 2.76	11.59
E	- 0.61	0.60	9.19	0.95	- 0.35	- 5.68	11.60
H	- 0.51	0.62	10.15	0.94	- 0.32	- 4.36	11.24
J	- 0.35	0.71	12.20	1.00	- 0.29	- 3.24	12.17
M	- 0.30	0.69	12.16	0.95	- 0.26	- 2.52	11.41
Q	- 0.34	0.85	10.78	1.17	- 0.32	- 4.36	11.87
U	- 0.09	0.76	13.67	0.97	- 0.21	- 1.48	11.98
Y	- 0.47	0.65	10.31	0.96	- 0.31	- 3.92	10.96
Z	- 0.44	0.67	11.58	0.98	- 0.31	- 3.92	12.23

TABLE VI

Cluster Members NGC 6704

Star	U-B	B-V	V	E(B-V)	$(B-V)_o$	M_v	V_o-M_v
1	0.00	0.52	12.42	0.65	- 0.13	- 1.10	11.18
2	- 0.33	0.49	12.23	0.72	- 0.23	- 1.88	11.77
3	0.03	0.55	12.59	0.67	- 0.12	- 0.56	10.81
4	- 0.03	0.54	13.01	0.68	- 0.14	- 0.74	11.41
5	- 0.09	0.54	13.30	0.70	- 0.16	- 0.56	11.52
6	- 0.08	0.54	13.10	0.70	- 0.16	- 0.56	11.32
11	0.12	0.57	14.33	0.67	- 0.10	+ 0.42	11.57
16	- 0.11	0.55	12.84	0.72	- 0.17	- 0.74	11.24
21	- 0.14	0.45	13.12	0.60	- 0.15	- 0.38	11.08
22	0.04	0.55	14.03	0.67	- 0.12	+ 0.10	11.59
28	0.19	0.63	14.26	0.72	- 0.09	+ 0.53	11.39
53	0.24	0.60	14.17	0.66	- 0.06	+ 0.26	11.57
54	0.08	0.52	12.89	0.62	- 0.10	- 1.10	11.65
68	0.47	0.80	15.14	0.84	- 0.04	+ 1.05	11.58
71	0.28	0.64	14.82	0.70	- 0.06	+ 0.86	11.62
74	0.11	0.65	14.05	0.77	- 0.12	+ 0.10	11.61
76	- 0.13	0.56	13.08	0.74	- 0.13	- 0.92	11.66

Figures 22 and 23

Figure 22 is the V_o, $(B-V)_o$ diagram for NGC 6604.
The solid line is the ZAMS corrected for the adopted values of reddening, absorption, and a distance modulus of 11.62 mag. Only cluster members are plotted. Open squares are stars observed by Moffat and Vogt, solid square is HD 167971, solid dots are other likely cluster members. A lower-case 'v' indicates a possible variable, as mentioned in the text.
Figure 23 is the V_o, $(B-V)_o$ diagram for NGC 6704. The solid line is the ZAMS corrected for the adopted values of reddening, absorption, and a distance modulus of 11.45 mag. Only probable cluster members are shown, with symbols the same as in Figure 14.

Figure 22

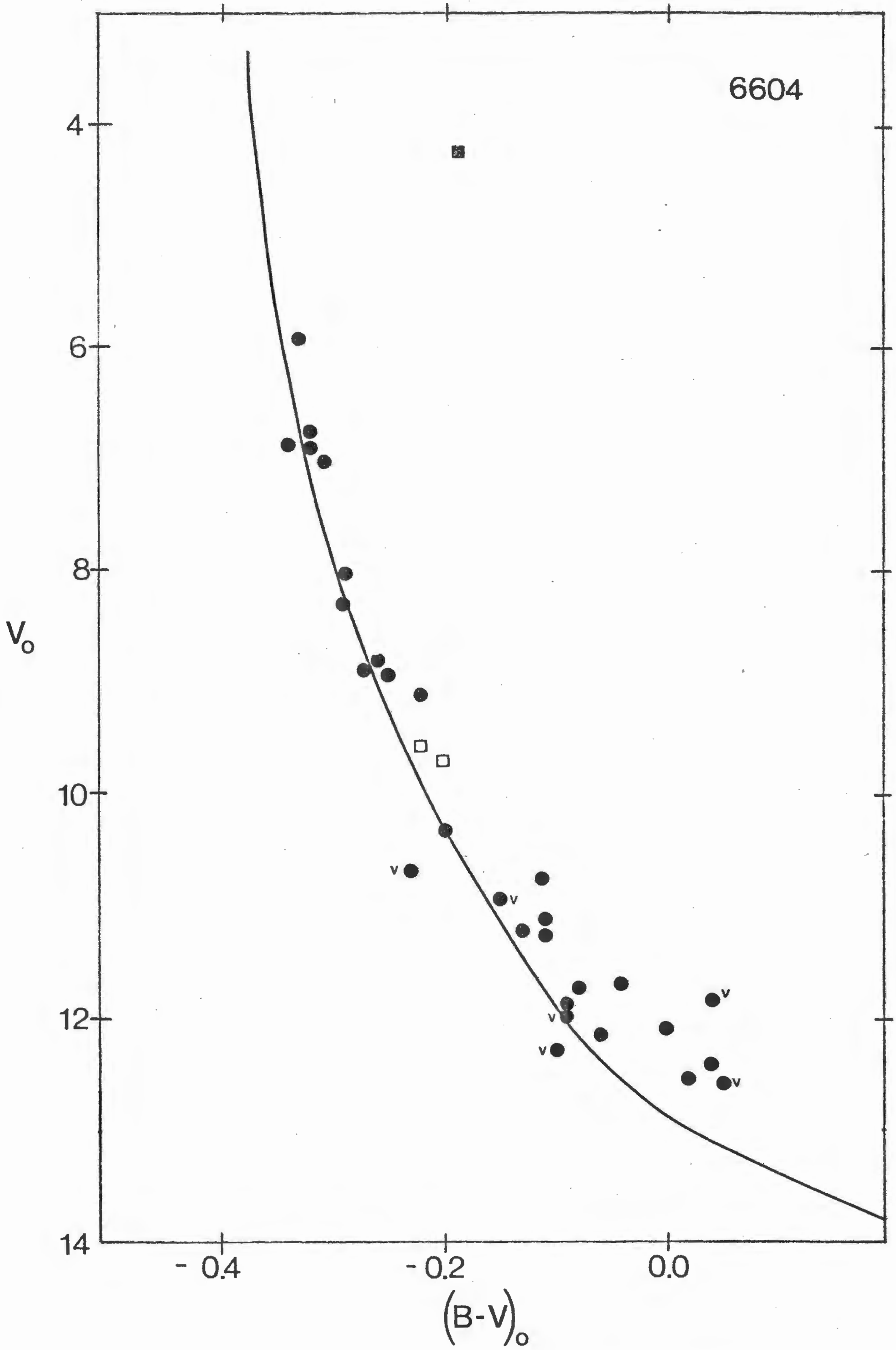

Figure 23

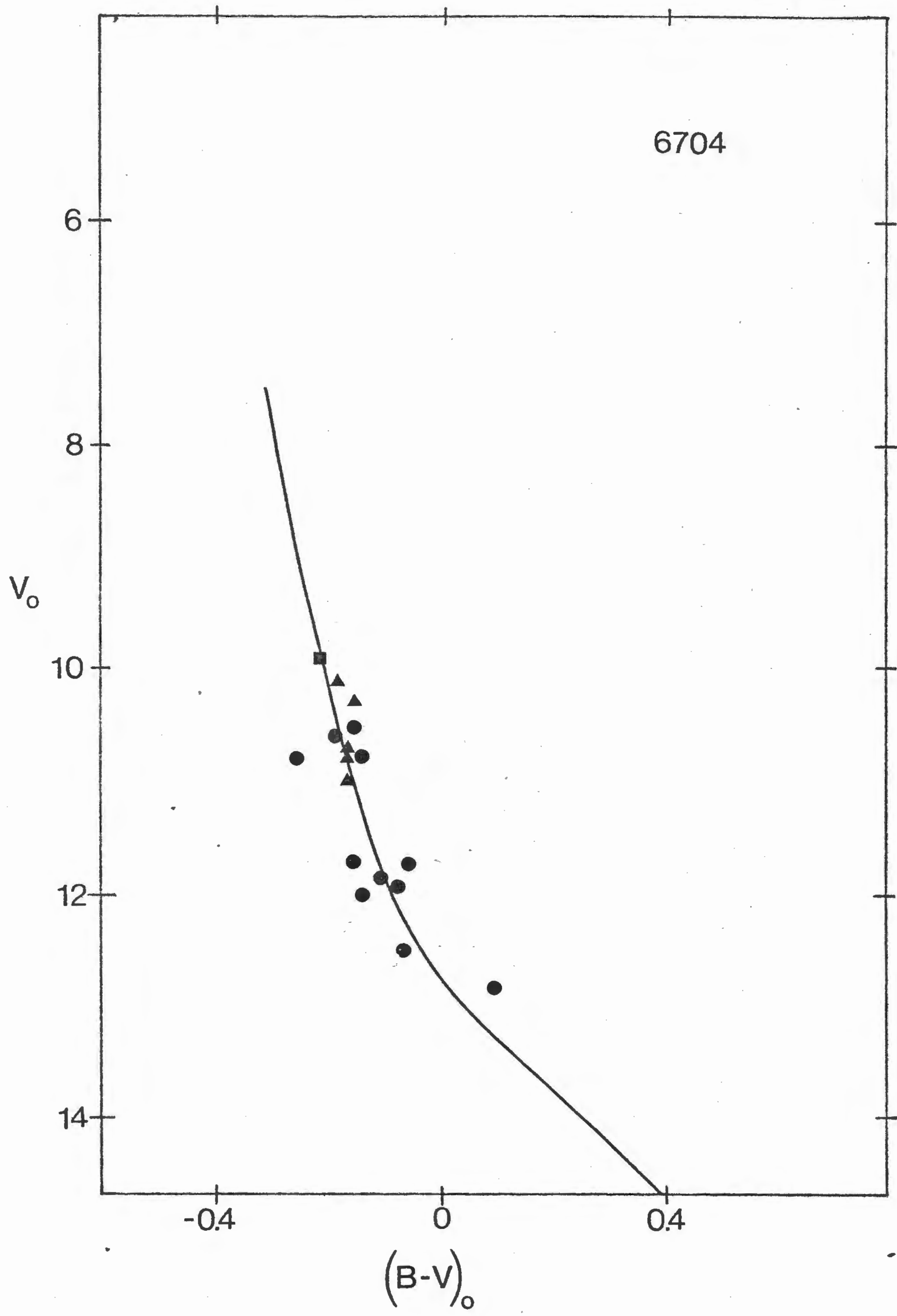

V.) COLOUR-MAGNITUDE DIAGRAM

4.1 NGC 6604

The colour-magnitude diagram of NGC 6604 reveals a well-defined main sequence extending from $V_o \sim 6$ to ~ 13. The scatter of points about the ZAMS is rather small, particularly in the bright end where photoelectric values dominate; the fainter portion of the main sequence tends to rise above the ZAMS by about 0.75 magnitudes. There is an apparent gap in the distribution along the ZAMS of about 1 magnitude at $V_o \sim 10$; this gap is probably due to the small number of stars observed. Two additional stars, both members and a close pair, were observed by Moffat and Vogt (1975). The UBV data from this source were plotted on the CMD for these two stars, which are seen to fill the apparent gap. These stars were not measured photographically because of their small separation on the plates and in the sky.

The central star of the cluster, HD 167971 (O8f Ia) was also observed by Moffat and Vogt and their results have been added to the CMD as well. This star was not observed photoelectrically in this study because of the lack of observing time caused by poor weather; the large size of the image and the diffraction spikes present on the plates prevented photographic photometry. The location of this star in the CMD is not unexpected for a slightly evolved blue supergiant with an emission-line spectrum.

The presence of several OB-type stars and a bright upper main sequence suggests that this cluster is a young object. The age of an open cluster can be estimated from several methods.

Age determinations of clusters are generally based on one of the parameters associated with the turnoff of massive stars from the main sequence towards the red giant stage of evolution. In principle, the "turn-on" point, or intersection of pre-main-sequence stars with the main sequence, can also be used to estimate cluster age. This has not been attempted here, because of possible spread in the formation time of stars in the cluster, and because uncertainties are larger in cluster membership and photometric calibration at the pre-main-sequence point (the pre-main-sequence envelope will be discussed below).

Allen (1973) gives three indicators of age, all based on observational parameters of the turnoff point: star(s) with: i) the most luminous absolute magnitude M_V, ii) the bluest $(B-V)_o$ colour index, and iii) the earliest spectral type on the main sequence. The most luminous absolute magnitude on the ZAMS is - 5.7. Interpolation in the table of Allen implies an age of 2.7×10^6 years. The bluest $(B-V)_o$ is - 0.35, indicating an age of less than 1×10^6 years. The earliest spectral type on the ZAMS (star E) is B0, with a resulting age estimate of 5.6×10^6 years.

Schlesinger (1969, 1972) obtained two relations involving mass, luminosity, and stellar age from the theoretical evolutionary tracks of Iben (1965):

$$\log L = -0.13 + 5.54(\log M) - 1.62(\log M)^{1.5}$$

$$\log \tau = 9.56 - 4.06(\log M) + 1.57(\log M)^{1.5}$$

where τ is the time scale for core-hydrogen burning (i.e. nuclear main sequence age). These equations were solved for $\bar{M}$ and log τ using the absolute magnitudes M_v of seven photoelectrically observed members, and the bolometric corrections given in Schlesinger's Table 2 (1969). The resulting mean value of log τ is 6.52 $\pm$ 0.24 (s.d.), corresponding to an age of $3.3 \pm 0.1 \times 10^6$ years.

The age estimates from Allen's three methods were each given a weight of one, while the age estimate from Schlesinger's method was given a weight of three. A weighted mean age of 3.4×10^6 years with a standard error of the weighted mean of 1.7×10^6 years was found. If the age found from the bluest $(B-V)_o$ is omitted (as it is the lowest value), the resulting weighted mean age is $4 \times 10^6 \pm 1.4 \times 10^6$ years. The value of 4 million years will be adopted here on the basis of the data presently available.

An age of 4 million years, if correct, would make NGC 6604 one of the youngest observed open clusters. NGC 2264, a well-known young cluster, has an age of ~3 million years (Walker, 1956); NGC 6611 (M 16) is believed to be ~2 million years old (Walker, 1961). It may be of interest to note in passing that NGC 6604 lies very near NGC 6611. Figure 24 is reproduced from Vehrenberg's Atlas Stellarum to show the region around both clusters. The distance to both clusters is very similar (~2.1 kpc) (Allen, 1973). Sharpless (1953) has suggested a possible connection between the nebulosities surrounding the two clusters as seen on 48-inch Schmidt plates of the Hale Observatories.

The CMD's of NGC 6604, NGC 6611, and NGC 2264 are shown together in Figure 25 for comparison.

Apart from the fewer number of stars observed, NGC 6604 differs from the other two clusters in having a blue supergiant member, and a less-pronounced envelope of stars above the main sequence.

Concerning the O8f supergiant, one important question deserves consideration: Why is a slightly evolved supergiant (apparently) observed in this cluster and not in NGC 2264 or NGC 6611? On the most simple-minded level, the presence of the O8f star argues in favour of a slightly older cluster. In that respect, the four million years adopted above is not in disagreement. However, that four million years is sufficient for a massive star to evolve into a supergiant is suggested by the theoretical evolutionary tracks of Chiosi and Summa (1970). The influence of other factors (eg. abundance differences arising from position in the Galaxy) are outside the scope of this study.

The apparent envelope of stars near $(B-V)_o = 0$ about 0.75 magnitudes above the ZAMS in NGC 6604 could be the result of:

i) observational error (i.e. the V magnitudes systematically too bright) or;

ii) pre-main-sequence objects in the process of gravitational contraction.

The possibility of a systematic brightening of the photographically derived values of V must be considered, in light of the nature of the photographic calibration curves. Only one photoelectric sequence star, C (V = 15.43), defines the faint end of the calibration curves. If the photoelectric V magnitude of this

Figure 24

Reproduction from Vehrenberg's Atlas Stellarum, showing region around NGC 6604 and NGC 6611. Portion shown is lower right quadrant of chart centered on declination - 10°, right ascension $18^h\ 20^m$.

Figure 24

10°
18^h20

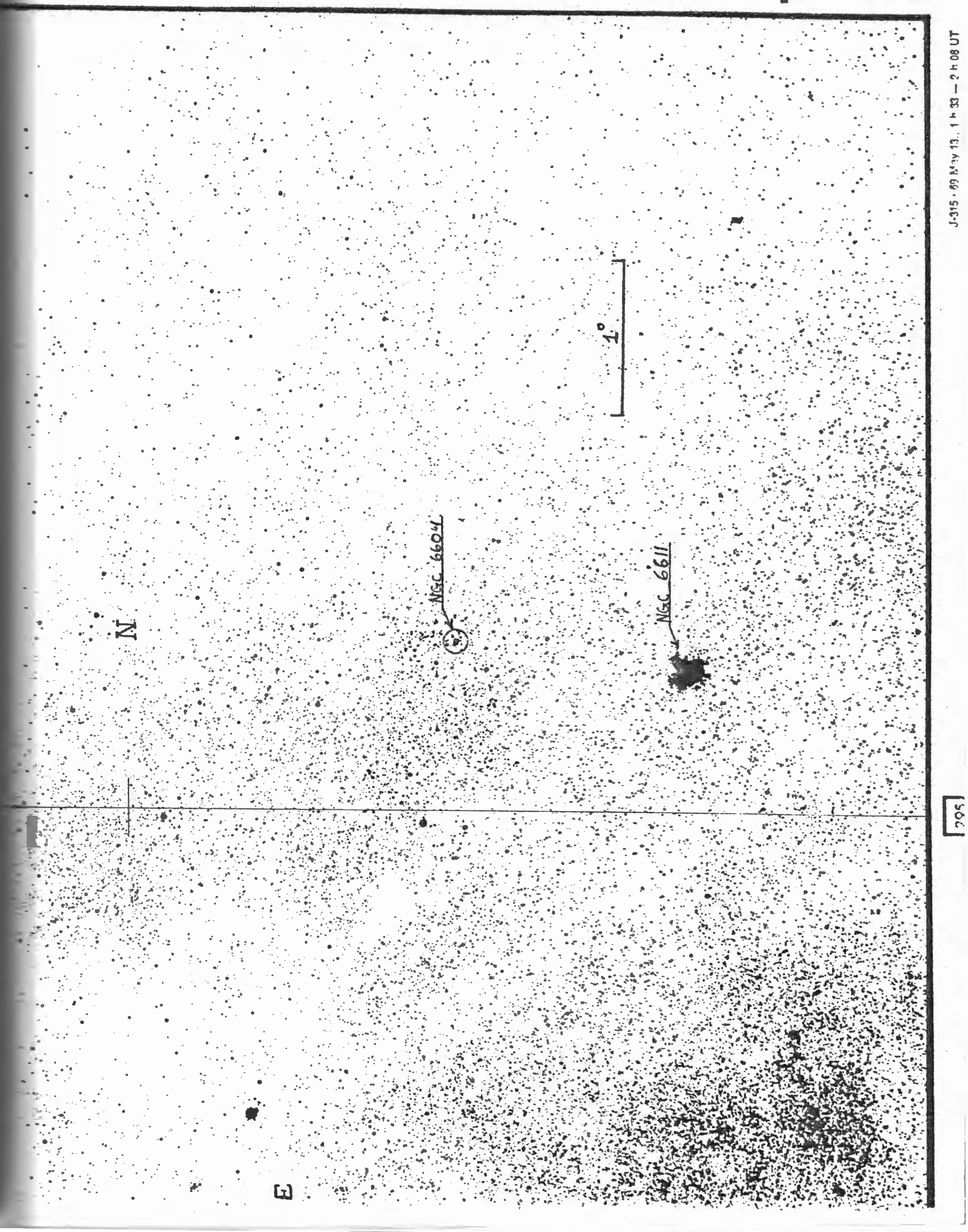

Figure 25

A comparison, to the same scale, of the V_o, $(B-V)_o$ diagrams of the young open clusters NGC 2264, NGC 6611, and NGC 6604. Solid line is the ZAMS corrected for the individual cluster values of reddening, absorption, and distance modulus.

Figure 25

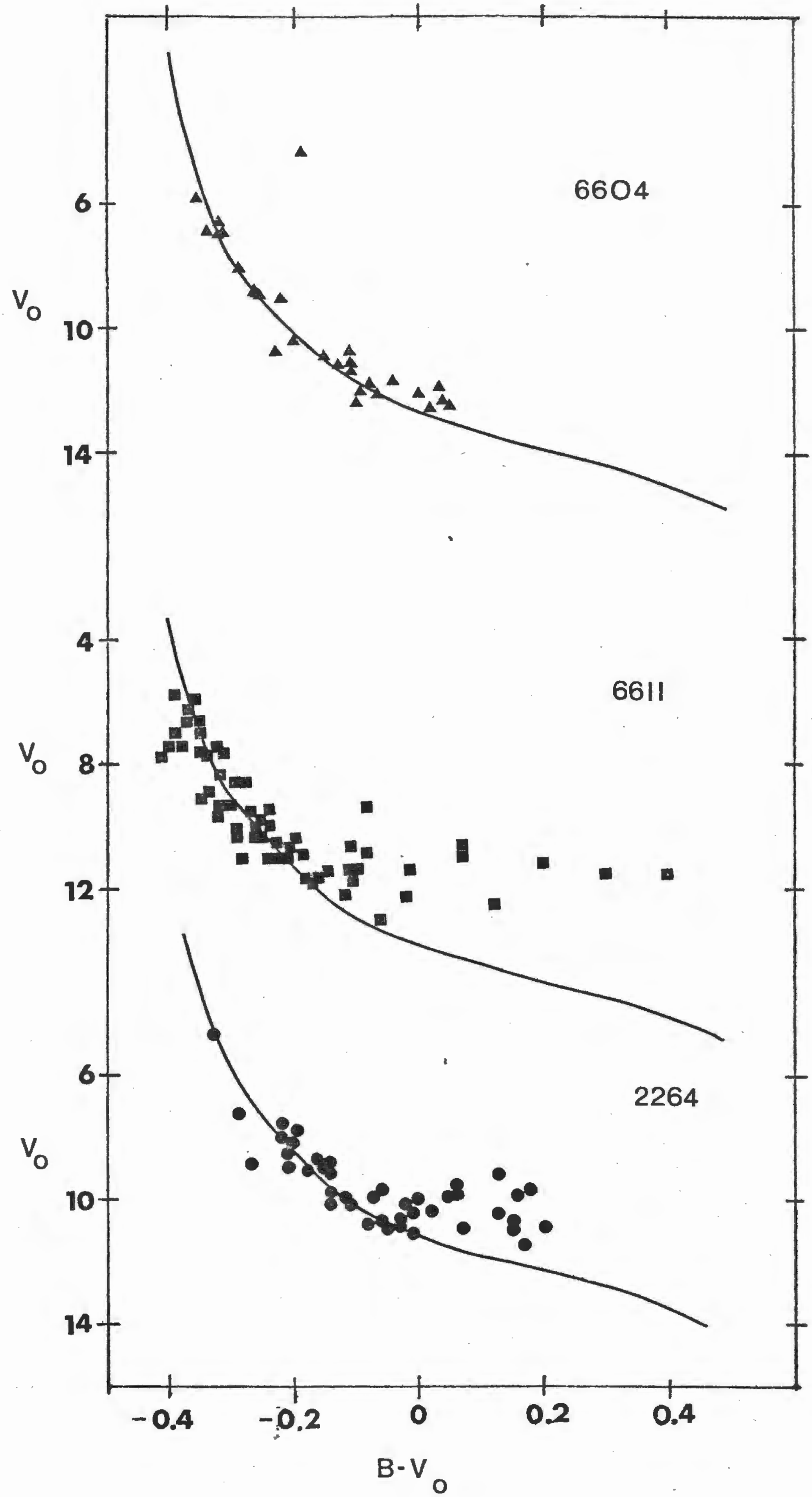

star is in error (too bright) it would tend to brighten the photographically-derived magnitudes of the fainter stars. To achieve an average brightening of 0.75 mag for stars fainter than $V = 15$ would require that the photoelectric V value be in error by at least one magnitude, due to the steep slope of the calibration curve as the plate limit is approached. An error of this magnitude, while not impossible, does seem improbable. (The next brightest star used in the calibration curve ($V = 13.61$) has a standard deviation in the photoelectric observations of $\pm$ 0.05 mag.)

It is therefore considered unlikely that a systematic error in the photographic photometry could account entirely for the observed envelope of stars above the ZAMS.

If the assumed age of 4 million years is correct, the theoretical pre-main-sequence tracks of Iben (1966) would indicate that stars of less than three solar masses would still be contracting to the main sequence. In terms of observational parameters, this would correspond to main sequence stars of spectral type A3 and later, or with $(B-V)_0 \geq +0.10$. However, stars are observed above the ZAMS as early as $(B-V)_0 \sim -0.05$. If these stars are indeed pre-main-sequence objects, a spread in the formation time of stars in the cluster is implied. An alternative explanation is that the apparent pre-main-sequence stars may indicate an age younger than the 4 million years suggested by the more usual methods which depend on the turnoff from the main sequence.

A spread in the formation time of stars in a cluster, such as mentioned above, has been suggested for other open clusters, such as NGC 6611 (Walker, 1961) and IC 348 (Strom, Strom, and Carrasco, 1974).

Several stars in the envelope above the ZAMS were noted as possible variables if the standard deviation of the mean V magnitude was significantly greater than the r.m.s. observational error. Without the means of making a blink comparator examination of the plate material, the variability of these faint stars cannot be confirmed here, although it would be in accord with observations of other very young clusters (Strom and Strom, 1973).

Two stars are located significantly below the ZAMS, and are not within a region of high E(B-V) as seen from Figure 16. If they are truly cluster members and have been de-reddened properly, their location in the CMD could be due to the obscuring effect of circumstellar shells of dust and gas, as would be expected in a region of youthful objects and known to contain appreciable amounts of gas (Tovmassian and Neressian, 1973). Observations in the infrared would be very useful for these stars.

It is tempting to search for similarities between NGC 6604 and other very young open clusters, however, one must distinguish between observation and speculation. There does appear to be an envelope of faint stars above the ZAMS, whose presence is in accord with pre-main-sequence evolutionary theory and observations of other young clusters; the important question as to whether the apparent pre-main-sequence nature of these stars, as well as the possible variability of others, is a consequence of their actual physical nature or a result of random scatter and observational error cannot be answered with any great certainty until a more detailed study of the cluster is made.

5.2 NGC 6704

The colour-magnitude diagram of NGC 6704 is rather straightforward in appearance; a fairly well-defined main sequence extending through a V_o range of 9.5 to 13. The scatter about the ZAMS is greater than the similar scatter in the CMD of NGC 6604. This is probably the result of the higher uncertainty involved in the transformations between the RGU and UBV photometric systems described earlier.

The brightest member of the cluster is the eclipsing binary system FN Sct, for which Bakos (1950) gives a period of $4^{d}.167153$ and a range in photographic magnitudes of 13.1 to 15.2 mag. No attempt was made to verify the period from photographic measures.

The age of the cluster was estimated using the same methods outlined for NGC 6604. With the four methods given the same weights as before, a weighted mean age of $2.1 \times 10^7 \pm 0.5 \times 10^7$ years is estimated. This age is about the same as that given by Allen (1973) for the open cluster NGC 1960 (M 35). The Atlas of Open Cluster Colour-Magnitude Diagrams of Hagen (1970) contains a CMD for NGC 1960, which upon examination resembles the CMD of NGC 6704, with the exception of three giant members present in NGC 1960. If the age estimated for NGC 6704 is correct, the theoretical work of Iben (1965) would indicate that a number of evolved stars should be observed in that cluster; no such stars were selected as probable members. The total number of stars in NGC 6704 may, of course, play a role. In view of the preliminary nature of the membership criteria as mentioned in the section on cluster membership, it is possible that some evolved stars which are actually cluster members have not been recognized as such.

6. RELATION TO LOCAL SPIRAL STRUCTURE

Both NGC 6604 and NGC 6704 are young enough to meet Schmidt-Kaler's (1971) age criterion for optical spiral tracers, so they may be added to a plot of the distribution of other spiral tracers, making use of the known galactic longitudes and the distances as determined in this study. Figure 26 shows the distribution of associations, clusters, and H II regions with supergiant members reproduced from Humphreys (1976). The locations of the two clusters are indicated.

Both clusters lie within the -I (Sgr) arm; NGC 6604 roughly centered in the arm, and NGC 6704 near the outer edge of the arm, closest to the Sun. It is of interest to note, without attaching any great significance to the point, that the ages and locations of the two clusters within the arm as well as the H II region associated with NGC 6604, are in agreement with the predictions of the spiral density-wave theory (Lin and Shu, 1964), where the more youthful objects and regions of gas excited by O and early B stars (H II regions) are expected to lie closer to the location of a density wave where star formation is initiated. This would mean the more youthful objects would lie nearer the inner edge of a spiral arm, if the pattern speed is less than the material speed, as is predicted for the Milky Way in the region of the Sun.

The proximity of NGC 6604 and NGC 6611, and their similar ages, raises the question of a possible connection between these clusters. Sharpless (1965) considered NGC 6604 to be the only cluster connected with the OB-association Ser OB 2, although an apparent connection between the nebulosity surrounding NGC 6604, NGC 6611, and NGC 6618 (M 17) was noted earlier by Sharpless (1953).

A number of bright clusters and H II regions lie in the general direction of NGC 6604 and NGC 6704; this is the result of looking tangentially along the -I arm in this direction at objects spread out along the line of sight. This point is important to the investigation of spiral structure by means of optical spiral tracers, for the distance alone is then the primary means of determining the nature of the -I arm within this narrow range of galactic longitude ($\ell = 20°-40°$).

Figure 26

Distribution on the galactic plane of associations (open circles), clusters (solid dots), and H II regions (open triangles) with supergiant members reproduced from Humphreys (1976). Locations of NGC 6604 and NGC 6704 are indicated by large solid circles.

Figure 26

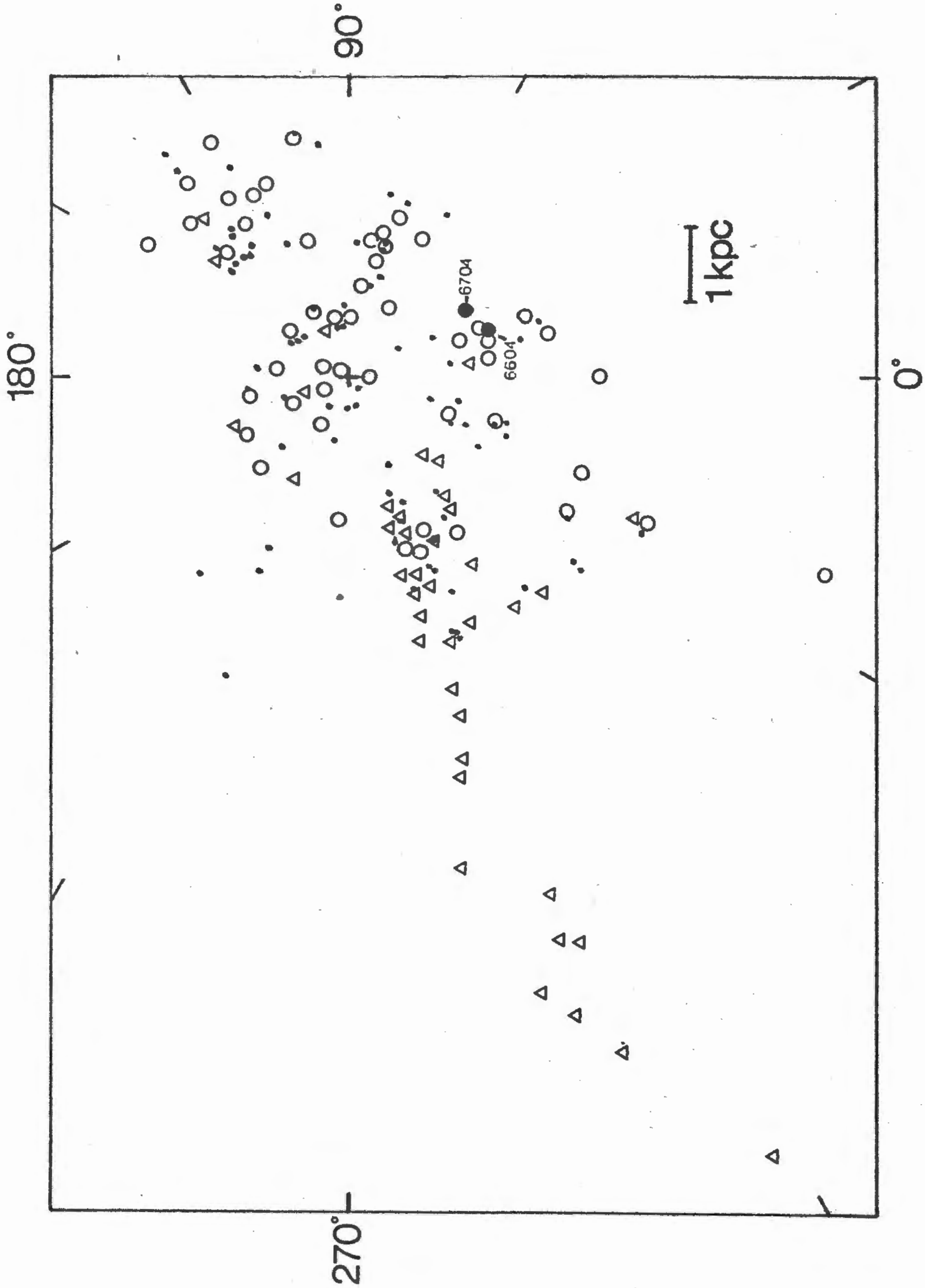

7.) CONSIDERATIONS FOR FUTURE WORK

Clearly, the observations of only two spiral tracers should not be expected to cast a great deal of new light on the problem of the local spiral structure in the region of galactic longitudes 20° - 70°. The heavy obscuration, along with the fact that we are looking tangentially along the -I arm in this direction, makes the discovery and study of optical spiral tracers difficult and uncertain. Moreover, it could be argued that the ability of radio astronomy to probe to great distances virtually unhindered by interstellar absorption makes the optical techniques less useful. However, the two methods of observation can clearly complement one another. The spiral structure in the region ℓ = 20°-70° is of great importance in determining the relation between the local (Orion) spiral feature and the -I (Sgr) arm; a search for and study of distant ($r \geq 2$ kpc) optical spiral tracers is surely worth the effort involved.

Aside from its usefulness as a tracer of spiral structure, the apparent youthful nature of NGC 6604 makes it an inherently interesting object, one that deserves a much more detailed study. Several aspects require particular attention:

i) confirmation of the pre-main-sequence nature of stars with $(B-V)_o \geq -0.05$;

ii) establishment of cluster membership with greater certainty;

iii) search for stars with peculiar features generally associated with clusters with ages around 2-4 million years; and

iv) a uvby-Hβ study, for luminosity and distance estimates.

A photometric study of the cluster down to a limiting magnitude of $V \sim 18^m$ would be necessary to confirm or deny the existence of pre-main-sequence objects. The use of infrared measurements would be helpful in determining which stars may have circumstellar shells and the true luminosities of these stars. A detailed photometric study would also serve to more firmly establish the values of reddening and distance modulus, particularly if UBV and uvby-Hβ was obtained.

Spectroscopic observations, both for classification purposes and the determination of radial velocities, would allow the search for peculiar stars to be made, to more firmly establish cluster membership.

Such a photometric and spectroscopic investigation, accompanied by a blink comparator examination of the cluster field to search for variability, would be the next logical step in resolving some of the questions raised here concerning the nature of NGC 6604.

8.) SUMMARY

The open clusters NGC 6604 and NGC 6704 have been studied in some detail with UBV photoelectric and photographic photometry, resulting in improved distance estimates and colour-magnitude diagrams.

The improvement in distances allows the two clusters to be used more reliably as tracers of spiral structure. Both clusters are found to lie within the -I (Sgr) arm, but are not sufficient in themselves to yield any new information about the extent of the -I arm in the direction of galactic longitude ℓ=20° - 70°; a survey of distant ($r \geq 2$ kpc) optical spiral tracers in this direction is clearly required to resolve several questions about the relationship between the -I arm and the local spiral feature.

NGC 6704 is a moderately young open cluster (~20 million years old) with 17 probable members observed in this study, including the eclipsing binary system FN Sct. The colour-magnitude diagram shows a well-defined main sequence, but no giant members are observed; they would, however, be expected from the age of the cluster. The distance to NGC 6704 is 1.95 ± 0.23 kpc, at galactic coordinates b= - 2.2°, ℓ = 28.2°. The total visual absorption is 2.34 magnitudes.

NGC 6604 is a very young (~4 million years old) cluster with 29 observed probable members, located at ℓ = 18.3°, b= + 1.7°, at a distance of 2.11 ± 0.40 kpc. The total visual absorption is 3.17 magnitudes. The colour-magnitude diagram shows a bright, well-defined main sequence; the central star of the cluster,

HD 167971, is an O8f supergiant which appears to have evolved slightly away from the zero-age main-sequence. The fainter stars with $(B-V)_o \geq -0.05$ appear to lie above the ZAMS and may be pre-main-sequence stars still in the process of gravitational contraction (this result must be confirmed, because of slight uncertainty in the photometric calibration near $V \sim 16$). Two stars are also observed to lie significantly below the ZAMS; for clusters of this age, this may be caused by circumstellar shells of gas and dust, as seen in NGC 2264.

References

Allen, C.W. 1973, Astrophysical Quantities (3rd Edition), Univ. of London, The Athlone Press.

Alter, G., Ruprecht, J., and Vanýsek, J. 1970, Catalogue of Star Clusters and Associations (2nd Edition), ed. G. Alter, B. Balazs, and J. Ruprecht, Akademiai Kiadó, Budapest.

Baade, W., and Mayall, N.U. 1951, Problems of Cosmical Aerodynamics (Dayton, Ohio: Central Air Documents Office), p. 165.

Bakos, G.A. 1950, Leiden Ann., 20, Nr. 4.

Becker, W. 1963, in Basic Astronomical Data; Stars and Stellar Systems, Vol. III, ed. K. Aa. Strand, Univ. of Chicago Press, p. 241.

Becker, W., and Fenkart, R. 1970, in The Spiral Structure of Our Galaxy, I.A.U. Symp. No. 38, ed. W. Becker and G. Contopoulos, D. Reidel Publ. Co., Dordrecht, Holland, p. 205.

Becker, W., and Stock, J. 1954, Zs. f. Ap., 34, 1.

Blaauw, A. 1963, in Basic Astronomical Data; Stars and Stellar Systems, Vol. III, ed. K. Aa. Strand, Univ. of Chicago Press, p. 383.

Bok, B.J. 1970, in The Spiral Structure of Our Galaxy, I.A.U. Symp. No. 38, ed. W. Becker and G. Contopoulos, D. Reidel Publ. Co., Dordrecht, Holland, p. 457.

Chiosi, C., and Summa, C. 1970, Astrophys. and Sp. Sci., 8, 478.

Crawford, D.L., and Mandwewala, N. 1976, Pub. A.S.P., 88, 917.

DuPuy, D.L. 1972, Ph.D thesis, University of Toronto, Toronto, Ontario.

Fernie, J.D. 1976, Pub. A.S.P., 88, 969.

FitzGerald, M.P., and Moffat, A.F.J. 1974, A.J., 79, 873.

Georgelin, Y.P., and Georgelin, Y.M. 1970, Astr. and Ap., 6, 349.

Golay, M. 1974, Introduction to Astronomical Photometry, D. Reidel Publ. Co., Dordrecht, Holland.

Grubbisich, C. 1965, Zs. f. Ap., 60, 249.

Gutiérrez-Moreno, A. 1975, Pub. A.S.P., 87, 805.

Hagen, G.L. 1970, Pub. David Dunlap Obs., 4.

Hardie, R. 1962, in Astronomical Techniques; Stars and Stellar Systems, Vol. II, ed. W.A. Hiltner, Univ. of Chicago Press, p. 178.

Herbst, W. 1975, A. J., 80, 498.

Hiltner, W.A., and Johnson, H.L. 1956, Ap. J., 124, 367.

Humphreys, R. 1976, Pub. A.S.P., 88, 647.

Iben, I. Jr. 1964, Ap. J., 140, 1631.

Johnson, H.L. 1958, Lowell Obs. Bull., 4, 37 (No. 90).

------------. 1960, ibid., 5, 17 (No. 107).

Johnson, H.L., and Morgan, W.W. 1953, Ap. J., 117, 313.

Johnson, H.L., Sandage, A.R., and Wahlquist, H.D. 1956, Ap.J., 124, 81.

Kukarkin, B.V., Kholopov, P.N., Efremov, Yu. N., Kukarkina, N.P., Kurochkin, N.E., Medvedeva, G.I., Perova, N.B., Fedorovich, V.P., and Frolov, M.S. 1969, General Catalog of Variable Stars (3rd Edition), The Academy of Sciences of the U.S.S.R., Moscow.

Kukarkin, B.V., Kholopov, P.N., Efremov, Yu. N., Kukarina, N.P., Kurochkin, N.E., Medvedeva, G.I., Perova, N.B., Pskovsky, Yu. P., Fedorovich, V.P., and Frolov, M.S. 1974, Second Supplement to the Third Edition of the General Catalogue of Variable Stars, The Academy of Sciences of the U.S.S.R., Moscow.

Landolt, A.U. 1973, A.J., 78, 959.

Lin, C.C., and Shu, F.H. 1964, Ap.J., 140, 646.

Lynds, B.T. 1962, Ap.J. Suppl., 7, No. 64, 1.

----------. 1968, in Nebulae and Interstellar Matter; Stars and Stellar Systems, Vol. VII, ed. B.M.Middlehurst and L.H. Aller, Univ. of Chicago Press, p. 119.

McCuskey, S.W. 1970, in The Spiral Structure of Our Galaxy, I.A.U. Symp. No. 38, ed. W. Becker and G. Contopoulos, D. Reidel Publ. Co., Dordrecht, Holland, p. 189.

Miller, S. 1968, Ap. J., 151, 473.

Moffat, M.P., and Vogt, N. 1975, Astr. and Ap. Suppl. Ser., 20, p. 160.

Morgan, W.W, Sharpless, S., and Osterbrock, D.E. 1952, A.J., 57, 3.

-----------, Whitford, A.E., and Code, A.D. 1953, Ap.J., 118, 318.

Racine, R. 1974, A.J., 79, 472.

Rohlfs, K. 1967, Z. f. Ap., 66, 225.

Sandage, A.R. 1975, Pub.A.S.P., 87, 853.

Schlesinger, B.M. 1969, Ap.J., 157, 533.

----------------. 1973, A.J., 77, 584.

Schmidt-Kaler, Th. 1971, in The Structure and Evolution of the Galaxy, ed. L.N. Mavridis, D. Reidel Publ. Co., Dordrecht, Holland, p 85.

Sharpless, S. 1953, Ap.J., 118, 362.

------------. 1965, in Galactic Structure; Stars and Stellar Systems, Vol. V, ed. A Blaauw and M. Schmidt, Univ. of Chicago Press, p. 131.

Stephenson, C.B., and Sanduleak, N. 1970, Catalogue of Luminous Stars in the Southern Milky Way, Pub. Warner & Swasey Obs, Cleveland, Ohio.

Strom, S.E., and Strom, K.M. 1973, Sky & Tel, 42, 279.

Strom, S.E., Srom, K.M., and Carrasco, L. 1974 Pub. A.S.P., 86, 798.

Tovmassian, H.M., and Neressian, S.E. 1973, Aus. Jour. Phys., 26, 861.

van Altena, W.F. 1974, Pub. A.S.P., 86, 217.

Walker, M.F. 1956, Ap. J. Suppl., 2, 365 (No. 23).

-----------. 1959, Ap. J., 130, 57.

-----------. 1961, ibid., 133, 438.

Walker, G.A.H. 1965, Ap. J., 141, 660.

APPENDICES I and II

Giving the photographically-derived UBV magnitudes and colours of stars within a circle of radius 5 arc-minutes centered on the centre of each cluster. In Appendix II, stars 1 through 50 were measured by Grubbisich in the RGU system; the magnitudes and colours given in the Appendix are the UBV equivalents of Grubbisich's measures. In the column headed 'Notes', the lower case letters 'm' and 'b' denote that the star is a probable member of the cluster, or a visual binary, respectively. A semi-colon following a magnitude or colour indicates that that value is uncertain.

APPENDIX I

UBV Magnitudes and Colours of Stars Near NGC 6604

Star	U-B	B-V	V	Notes
1	1.50:	0.08	15.46	
2	----	0.85	15.69	
3	----	----	15.60	
4	----	1.62	14.34	
5	----	1.18	15.66	
6	----	----	15.04	
7	0.16	0.58	13.74	
8	- 0.09	0.52	13.93	
9	0.17	0.48	15.77	
10	0.66	0.50	14.74	
11	0.01	0.52	13.98	
12	----	0.79	15.98	
13	----	1.49:	15.56	
14	1.14	1.41	13.64	
15	0.11	0.61	14.70	
16	- 0.07	0.59	13.90	
17	----	0.67	15.74	
18	0.07	0.51	14.05	
19	0.11	0.62	12.85	
20	----	0.81	15.57	
21	0.53:	0.98	15.83	m
22	----	1.35:	15.72	
23	0.30	0.47	15.25	
24	----	----	15.96	
25	0.07	0.53	14.75	
26	----	0.88	15.83	
27	0.08	0.52	14.08	
28	0.77:	0.51:	14.29:	
29	1.13:	0.88	14.99	m
30	----	0.56	16.04	

Star	U-B	B-V	V	Notes
31	0.36	0.53	14.38	
32	----	0.71	15.71	
33	- 0.23	0.61	13.12	
34	0.87	0.77	15.34	
35	0.19	0.47	13.80	
36	----	0.83	16.00	
37	----	----	15.20	
38	0.57	0.48	14.97	
39	0.14	0.57	14.00	
40	0.43	0.92	14.97	m
41	0.28	0.29	15.22	
42	----	----	15.42	
43	0.37	0.69	14.83	
44	----	1.80	14.41	
45	0.38	1.03	14.01	
46	0.75:	0.85	14.53	m
47	----	1.15:	15.85	
48	----	1.16	15.47	
49	0.74	0.76	14.78	
50	0.11	0.81	14.21	m
51	0.17	0.55	14.40	
52	0.51	0.74	14.84	
53	- 0.06	1.00	13.95	
54	----	----	15.76	
55	----	1.08	15.24	
56	0.04	0.83	14.48	m
57	0.04	0.47	14.28	
58	0.15	0.85	14.03	m
59	----	1.36:	15.44	
60	----	0.86	15.72	
61	- 0.21	0.74	12.38	m
62	1.13	1.97	12.21	
63	0.55	0.99	14.83	
64	0.30	0.70	13.94	

Star	U-B	B-V	V	Notes
65	----	1.01	15.82	m
66	0.51:	0.96	15.36	m
67	0.26	0.55	13.96	
68	0.58	0.53	14.68	
69	0.25:	0.86	15.55	m
70	0.09	0.36	14.21	
71	0.79	0.33	15.23	
72	----	0.82	15.84	
73	----	0.90	15.43	
74	----	0.87	15.24	m
75	----	0.97	15.37	
76	- 0.08	0.59	14.18	
77	0.37	0.63	14.77	
78	----	----	15.78	
79	----	1.00	15.68	m
80	0.00	0.85	14.39	m
81	----	0.72	15.71	
82	1.29	1.03	14.91	
83	0.04	0.70	14.41	
84	----	0.98	15.26	
85	0.50	0.69	12.13	
86	----	1.08	15.34	
87	- 0.11	0.73	13.94	m
88	0.38	0.83	14.07	
89	0.48:	1.00	15.10	m
90	0.47	0.87	15.14	m
91	- 0.26	0.86	11.91	m
92	1.30	1.45	12.99	
93	0.32	0.45	13.20	
94	0.07	0.59	14.52	
95	1.15:	1.41	14.47	

APPENDIX II

UBV Magnitudes and Colours of Stars Near NGC 6704

Star	U-B	B-V	V	Notes
1	0.00	0.52	12.42	m,b
2 (FN Sct)	- 0.33	0.49	12.23	m
3	0.03	0.55	12.59	m,b
4	- 0.03	0.54	13.01	m,b
5	- 0.09	0.54	13.30	m,b
6	- 0.08	0.54	13.10	m,b
7	0.04	0.85	14.68	
8	0.20	0.54	14.88	
9	- 0.01	1.10	14.89	
10	0.00	0.85	15.05	
11	0.12	0.57	14.33	m
12	----	----	-----	
13	- 0.23	1.03	15.04	
14	0.22	0.51	14.01	
15	0.01	0.74	12.69	
16	- 0.11	0.55	12.84	m
17	0.43	1.09	11.73	
18	0.25	0.72	14.74	
19	0.32	1.01	13.34	
20	0.89	1.68	13.54	
21	- 0.14	0.45	13.12	m
22	0.04	0.55	14.03	m
23	0.30	0.66	13.99	
24	0.10	0.74	14.45	
25	- 0.15	0.66	15.23	
26	- 0.15	0.71	14.78	
27	----	----	-----	
28	0.19	0.63	14.26	m
29	----	----	-----	
30	0.76	1.64	12.20	

Star	U-B	B-V	V	Notes
31	0.09	0.55	14.66	
32	- 0.06	0.61	15.14	
33	0.02	0.76	14.92	
34	0.36	0.65	15.25	
35	- 0.01	0.91	14.57	
36	- 0.19	0.72	14.56	
37	0.09	0.71	13.94	
38	0.49	0.89	14.44	
39	2.02	2.01	11.20	
40	----	----	-----	
41	0.15	0.52	14.65	
42	----	----	-----	
43	----	----	-----	
44	0.33	0.67	13.16	
45	----	----	-----	
46	0.54	1.13	14.09	
47	0.55	0.70	12.98	
48	0.43	1.89	14.09	
49	----	----	-----	
50	0.04	0.75	14.32	
51	0.15	0.63	15.02	
52	0.06	1.08	14.99	
53	0.24	0.60	14.17	m
54	0.08	0.52	12.89	m
55	0.11	1.40	14.46	
56	0.12	1.28	14.55	
57	0.80	0.93	13.73	
58	0.11	1.18	14.87	
59	----	1.76	14.37	
60	0.00	0.61	15.48	
61	----	1.95	14.20	
62	0.22	1.01	15.46	
63	0.09	0.92	15.50	

Star	U-B	B-V	V	Notes
64	----	2.17	14.00	
65	0.22	1.20	14.78	
66	- 0.11	0.77	15.57	
67	0.02	0.59	15.37	
68	0.47	0.80	15.14	m
69	----	1.88	14.49	
70	----	1.70	14.66	
71	0.28	0.64	14.82	m
72	0.13	0.71	14.71	
73	0.00	0.70	15.63	
74	0.11	0.65	14.05	m
75	0.02	0.69	15.29	
76	- 0.13	0.56	13.08	m
77	----	0.86	15.56	
78	----	2.44	13.46	

PLATE 1

NGC 6704

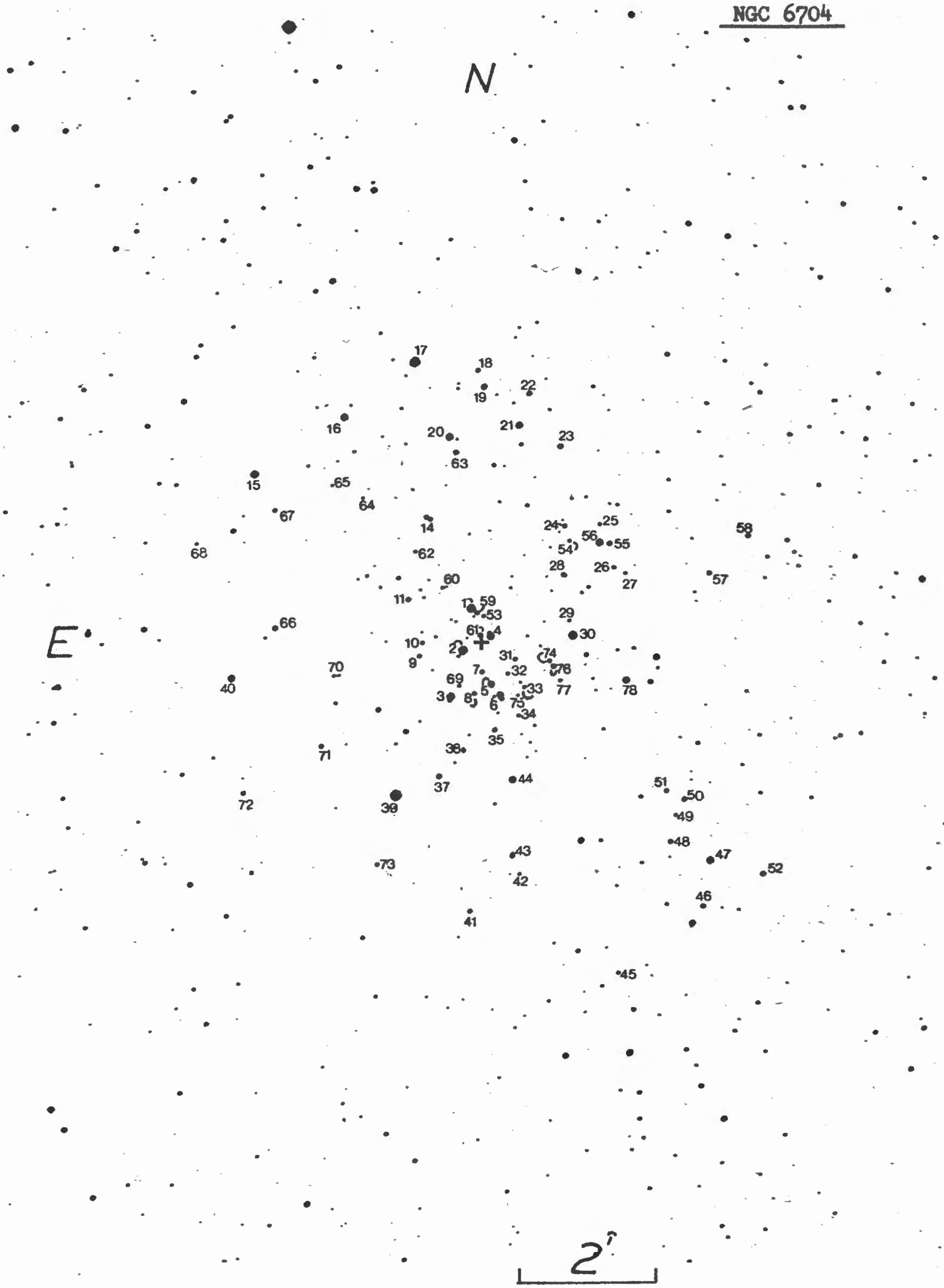

PLATE 2

NGC 6604